Transient wheel-rail rolling contact theories

(article starts on next page)

Transient wheel-rail rolling contact theories

Luigi Romano[*a], Michele Maglio[a], and Stefano Bruni[b]

[a]Department of Mechanics and Maritime Sciences, Chalmers University of Technology, Hörsalsvägen 7A, 412 96 Gothenburg, Sweden
[b]Dipartimento di Meccanica, Politecnico di Milano, Milan, Italy

Abstract

This paper provides an overview of different theories to analyse unsteady rolling contact phenomena between wheel and rail: the exact formulation by Kalker, the simplified model based on the Winkler approximation, and the recent two-regime model. The classic solution to the transient problem derived by Kalker using the complete theory of elasticity is first recalled. The more involved situation of combined creepages and spin is analysed using Kalker's simplified model. Analytical solutions are reported in integral form concerning the time-varying and constant creepages. Qualitative results are additionally provided for the case of a time-varying contact patch. Finally, a novel theory, which describes the transient evolution of the force-creepage characteristics using a system of ordinary differential equations (ODEs), is introduced.

Keywords

Wheel-rail rolling contact; transient rolling contact; rail-wheel tribology; contact mechanics

1 Introduction

Despite a long tradition of research in rolling contact mechanics, transient phenomena[1] are still poorly comprehended from a theoretical viewpoint, and only a few scientific contributions are available in the literature concerned with the problem. Nonetheless, unsteady dynamics may be expected to play a crucial role in the excitation of instability behaviours and exacerbation of wear effects and fatigue [1–3], which motivates the need for a fundamental understanding. In this context, a first rigorous analysis was attempted in a famous series of papers by Kalker, who, using the complete theory of elasticity [4], restricted his investigations to similar elastic cylinders rolling over each other, and subjected to pure longitudinal creepage [5, 6]. The solutions derived by Kalker in his seminal works are regarded today as classic results in contact mechanics, and are reported by a number of authoritative books dealing with the subject [7–10]. However, the case of pure longitudinal creepage appears to be the only one admitting a closed-form solution. In fact, the intrinsic complexities connected with unsteady rolling have limited other exact analyses, e.g., concerning combined creepage conditions, to the numerical domain [11–14], whereas approximated solutions have been proposed by some scholars [15, 16]. According to Johnson [8], the more involved cases of combined creepages and spin may be studied, at least qualitatively, using Kalker's *simplified model* [7, 8, 17], which is essentially based on a Winkler approximation for the elastic relationship between deformations and stresses.

Interestingly, Kalker initially explored transient problems using the simplified formulation in [18], but then dismissed the results as trivial, asserting that the theory was uncapable of capturing unsteady dynamics. In spite of Kalker's claims [7], other scientists have found in Kalker's simplified theory an adequate theoretical framework to explain nonstationary effects in rolling contact, including instability phenomena connected to corrugation [19–24]. It is also worth observing that the simplified theory still constitutes the predominant approach to studying the transient behaviour of tyres in road vehicle

---

[*]Corresponding author. Email: luigi.romano@chalmers.se.
[1]With transient rolling contact, it is intended in this paper any type of rolling contact dynamics where a variable is possibly time-varying. These mainly include the effect of varying creepages, contact patch dimension and normal load (possibly induced by corrugation phenomena). Secondary aspects connected to variations in other operational or structural parameters like, e.g., temperature may also be considered, but have been disregarded in the present paper.

dynamics (where it is more commonly referred to as *brush theory* [25, 26]), and have been recently adapted to investigate other problems arising in rolling contact [27–29]. Indeed, a major strength of the simplified model is that, by replacing the complicated convolution integrals stemming from the theory of elasticity with linear algebraic relationships, it allows solving the transient problem for a vast combination of operating conditions of the wheel-rail system. Analytical solutions derived using the Winkler approximation are reported, for example, in [30–32]. Additional extensions to the model have also been presented recently in [33, 34] and [35], to cope with large spin creepages and omnidirectional rolling contact. In the present paper, the treatment of the transient rolling contact problem according to the simplified theory is based on the latest works authored by Romano [32, 34].

Kalker's simplified theory still describes the rolling contact problem using a distributed representation, that is, a system of partial differential equations (PDEs). In rail vehicle dynamics, on the other hand, where the focus is prevalently on stability analyses and simulation [36–38], unsteady rolling contact may be more conveniently represented using approximated models, formulated in terms of ordinary differential equations (ODEs). In [39], the derivation of such models was inspired by the fundamental understanding of the transient phenomena that may be qualitatively analysed using the simplified theory, as suggested by Johnson [8]. The resulting two-regime theory, introduced first in [31], allows to accurately describe the transient evolution of the force-creepage characteristics using a simplified system of (possibly nonlinear) ODEs. The main intuition behind the two-regime approach is that the PDEs governing the rolling contact dynamics may be approximated by two different systems of ODEs depending on the value of the rolling speed. In this paper, the two-regime theory developed for tyres is adapted to cover the interaction between the wheel and the rail. To this end, different formulae for the steady-state creepage-force laws are reviewed, and the corresponding two-regime models are derived accordingly. More specifically, the steady-state models considered in this paper are Carter's model [40], Kalker's linear model [4], and the formulation developed by Shen, Elkins and Hedrick [41, 42]. Such formulations constitute a novelty in the current research field. In fact, to the best of the authors' knowledge, the present investigation represents indeed the most complete reference on the subject of transient wheel-rail rolling contact, at least concerning the analytical treatment of the problem. In the very same context, the purpose of the two regime-formulation is twofold. In particular, its first ambition is to provide an approximated description, albeit sufficiently adequate, of transient rolling contact, allowing for a fundamental understanding of the salient phenomena connected with unsteady dynamics. Such a fundamental understanding is often prevented by the extreme complexity of the mathematical formulations adopted in the field of contact mechanics, where numerical methods are applied to solve transient problems. By providing a viable alternative to investigate unsteady effects, the two-regime theory may also be more easily integrated with complete vehicle models, and support the development of control or estimation algorithms. Therefore, the second purpose of the proposed formulation is to enable the modelling of transient wheel-rail rolling contact phenomena also in the context of railway dynamics studies, whereas the approximation of steady forces is currently standard.

The remainder of this paper is organised as follows. The governing PDEs of the rolling contact problem are introduced in Sect. 2, together with the main assumptions of the theory, the boundary and initial conditions. Sections 3 and 4 are dedicated to the analysis of the transient problem concerning the complete theory of elasticity and the simplified theory developed by Kalker, respectively. In particular, in Sect. 4, the stationary and transient solutions for the mutual tangential deformation between two contacting bodies is derived using the method of the characteristic lines considering constant and time-varying creepages. Qualitative results are also discussed concerning the case of a time-varying contact patch, which might be relevant when investigating, e.g., transient phenomena related to corrugation effects. The two-regime theory is then adapted to describe the wheel-rail interaction in Sect. 5. Section 6 compares the three theories for different operating conditions of the wheel-rail system. Finally, the main conclusions are drawn in Sect. 7, where some possible directions for future research are also outlined.

2 Transient theory of rolling contact

In this paper, the rolling contact problem between the wheel and the rail is studied considering a contact-fixed reference frame $(O; x, y, z)$ with unit vectors $(\hat{\boldsymbol{e}}_x, \hat{\boldsymbol{e}}_y, \hat{\boldsymbol{e}}_z)$. The contact takes place inside a small area, called contact patch, possibly time-varying and denoted here with $\mathscr{C} = \mathscr{C}(t)$ and modelled as a compact subset of $\mathbb{R}^2$, with boundary $\partial\mathscr{C} = \partial\mathscr{C}(t)$ and interior $\mathring{\mathscr{C}} = \mathring{\mathscr{C}}(t)$, where the governing PDEs of the model are prescribed[2]. In particular, the kinematic relationship describing the mutual deformation

---

[2]When the the contact patch is allowed to vary over time, the domain $\mathring{\mathscr{C}}_\infty \triangleq \cup_{t\in\mathbb{R}}\mathring{\mathscr{C}}(t) \times \{t\}$ is said to be *noncylindrical*.

of the two contacting bodies may be derived according to Kalker's approach, yielding

$$\boldsymbol{s}(\boldsymbol{x},t) = V(t)\big[\boldsymbol{\xi}(t) + \mathbf{A}_\phi(t)\boldsymbol{x}\big] + \frac{\partial \boldsymbol{u}_\tau(\boldsymbol{x},t)}{\partial t} + \boldsymbol{v}_\tau(\boldsymbol{x},t)\cdot\nabla_\tau\boldsymbol{u}_\tau(\boldsymbol{x},t), \qquad (\boldsymbol{x},t)\in\mathring{\mathscr{C}}\times\mathbb{R}_{>0}. \qquad (1)$$

In Eq. (1), $\nabla_\tau \triangleq [\partial/\partial x \; \partial/\partial y]^{\mathrm{T}}$ is the tangential gradient, $\boldsymbol{s}(\boldsymbol{x},t) = [s_x(\boldsymbol{x},t)\; s_y(\boldsymbol{x},t)]^{\mathrm{T}}$ is the relative slip, $\boldsymbol{u}_\tau(\boldsymbol{x},t) = [u_x(\boldsymbol{x},t)\; u_y(\boldsymbol{x},t)]^{\mathrm{T}}$ is the difference between the bodies' deformation inside the contact patch $\mathscr{C}$, $\boldsymbol{v}_\tau(\boldsymbol{x},t) = [v_x(\boldsymbol{x},t)\; v_y(\boldsymbol{x},t)]^{\mathrm{T}}$ is the rolling velocity, the vector $\boldsymbol{\xi}(t) = [\xi_x(t)\; \xi_y(t)]^{\mathrm{T}}$ collects the longitudinal and lateral creepages, and $\mathbf{A}_\phi(t)$ denotes the spin tensor, accounting for the spin creepage $\phi(t)$:

$$\mathbf{A}_\phi(t) = \begin{bmatrix} 0 & -\phi(t) \\ \phi(t) & 0 \end{bmatrix}. \qquad (2)$$

The definition of the spin tensor is not standard in the literature, but is used in this paper to provide a neat representation of the governing PDEs of the model. In particular, concerning the wheel-rail interaction, the rolling velocity reads $\boldsymbol{v}_\tau(\boldsymbol{x},t) = -V(t)\hat{\boldsymbol{e}}_x$, being $V(t) \triangleq \big\|\boldsymbol{v}_\tau(\boldsymbol{x},t)\big\|$ the scalar rolling speed, and therefore Eq. (1) simplifies to

$$\boldsymbol{s}(\boldsymbol{x},t) = V(t)\big[\boldsymbol{\xi}(t) + \mathbf{A}_\phi(t)\boldsymbol{x}\big] + \frac{\partial \boldsymbol{u}_\tau(\boldsymbol{x},t)}{\partial t} - V(t)\frac{\partial \boldsymbol{u}_\tau(\boldsymbol{x},t)}{\partial x}, \qquad (\boldsymbol{x},t)\in\mathring{\mathscr{C}}\times\mathbb{R}_{>0}. \qquad (3)$$

It is worth noticing that the two PDEs describing the longitudinal and lateral slip are uncoupled according to both the formulations (1) and (3).

In the most general form, the boundary (BC) and initial condition (IC) for the governing PDEs (3) of the rolling contact problem may be prescribed concerning the tangential stress vector $\boldsymbol{p}_\tau(\boldsymbol{x},t) = [p_x(\boldsymbol{x},t)\; p_y(\boldsymbol{x},t)]^{\mathrm{T}}$:

$$\text{BC:} \qquad \boldsymbol{p}_\tau(\boldsymbol{x},t) = \boldsymbol{0}, \qquad\qquad (\boldsymbol{x},t)\in\mathscr{L}\times\mathbb{R}_{>0}, \qquad (4)$$

$$\text{IC:} \qquad \boldsymbol{p}_\tau(\boldsymbol{x},0) = \boldsymbol{p}_{\tau0}(\boldsymbol{x}), \qquad\qquad \boldsymbol{x}\in\mathring{\mathscr{C}}_0. \qquad (5)$$

where $\boldsymbol{p}_{\tau0}(\boldsymbol{x}) = [p_{x0}(\boldsymbol{x})\; p_{y0}(\boldsymbol{x})]^{\mathrm{T}}$ is a known initial distribution for the tangential stresses, $\mathring{\mathscr{C}}_0 \triangleq \mathring{\mathscr{C}}(0)$ is the initial configuration of the interior of the contact patch, and $\mathscr{L} = \mathscr{L}(t)$ denotes the leading edge, collecting the points of the boundary $\partial\mathscr{C}$ where the material particles enter $\mathscr{C}$. More generally, if the boundary $\partial\mathscr{C}$ is sufficiently smooth, it may be decomposed as follows [32, 34]:

$$\mathscr{L} \triangleq \left\{\boldsymbol{x}\in\partial\mathscr{C} \;\middle|\; \big[\boldsymbol{v}_\tau(\boldsymbol{x},t) - \boldsymbol{v}_{\partial\mathscr{C}}(\boldsymbol{x},t)\big]\cdot\hat{\boldsymbol{n}}_{\partial\mathscr{C}}(\boldsymbol{x},t) < 0\right\}, \qquad (6a)$$

$$\mathscr{N} \triangleq \left\{\boldsymbol{x}\in\partial\mathscr{C} \;\middle|\; \big[\boldsymbol{v}_\tau(\boldsymbol{x},t) - \boldsymbol{v}_{\partial\mathscr{C}}(\boldsymbol{x},t)\big]\cdot\hat{\boldsymbol{n}}_{\partial\mathscr{C}}(\boldsymbol{x},t) = 0\right\}, \qquad (6b)$$

$$\mathscr{T} \triangleq \left\{\boldsymbol{x}\in\partial\mathscr{C} \;\middle|\; \big[\boldsymbol{v}_\tau(\boldsymbol{x},t) - \boldsymbol{v}_{\partial\mathscr{C}}(\boldsymbol{x},t)\big]\cdot\hat{\boldsymbol{n}}_{\partial\mathscr{C}}(\boldsymbol{x},t) > 0\right\}, \qquad (6c)$$

being $\boldsymbol{v}_{\partial\mathscr{C}}(\boldsymbol{x},t)$ the velocity of the boundary, and $\hat{\boldsymbol{n}}_{\partial\mathscr{C}}(\boldsymbol{x},t)$ the outward-pointing unit normal to $\partial\mathscr{C}$. The subsets $\mathscr{N}$ and $\mathscr{T}$ are referred to as *neutral* and *trailing edge*, respectively. Possibly, the initial distribution $\boldsymbol{p}_{\tau0}(\boldsymbol{x})$ should be a $C^1(\mathring{\mathscr{C}}_0;\mathbb{R}^2)$ function, satisfying the compatibility condition $\boldsymbol{p}_{\tau0}(\boldsymbol{x}) = \boldsymbol{0}$ on $\mathscr{L}_0 \triangleq \mathscr{L}(0)$. The BC in Eq. (4), together with the notion of leading edge as defined as in Eq. (6a), are *noncharacteristic* [43–45], at least according to Kalker's simplified theory.

The governing PDEs (3) are also complemented by the following two conditions for the stick and slip zone of the contact patch:

$$\big\|\boldsymbol{s}(\boldsymbol{x},t)\big\| = 0 \implies \big\|\boldsymbol{p}_\tau(\boldsymbol{x},t)\big\| \le \mu p_z(\boldsymbol{x}), \qquad (7a)$$

$$\big\|\boldsymbol{s}(\boldsymbol{x},t)\big\| > 0 \iff \boldsymbol{p}_\tau(\boldsymbol{x},t) = -\mu q_z(\boldsymbol{x})\frac{\boldsymbol{s}(\boldsymbol{x},t)}{\big\|\boldsymbol{s}(\boldsymbol{x},t)\big\|}, \qquad (7b)$$

where μ denotes the friction coefficient, as postulated by the simplest Coulomb-Amontons formulation. It should be observed that, according to more general models, like those discussed in [46–48], the friction coefficient may exhibit strong dependencies upon the operational parameters, including slip and temperature. However, such effects are disregarded in the present paper. Moreover, the influence of third body or viscoelastic layers [49] is also neglected. For a numerical treatment of general viscoelastic rolling contact problems, the reader is referred instead to [50, 51].

In any case, according to the previous inequalities (7), the stick and slip areas $\mathscr{C}^{(\mathrm{a})}$, $\mathscr{C}^{(\mathrm{s})}$ may thus be defined formally as the sets

$$\mathscr{C}^{(\mathrm{a})} \triangleq \big\{ \boldsymbol{x} \in \mathscr{C} \mid \text{Eq. (7a) holds} \big\}, \tag{8a}$$

$$\mathscr{C}^{(\mathrm{s})} \triangleq \big\{ \boldsymbol{x} \in \mathscr{C} \mid \text{Eq. (7b) holds} \big\}. \tag{8b}$$

Departing from the definitions in Eqs. (8), a generic quantity is sometime denoted in this paper by $(\cdot)^{(\mathrm{a})}(\boldsymbol{x})$ if $\boldsymbol{x} \in \mathscr{C}^{(\mathrm{a})}$, and by $(\cdot)^{(\mathrm{s})}(\boldsymbol{x})$ if $\boldsymbol{x} \in \mathscr{C}^{(\mathrm{s})}$.

It should be noticed that, in the transition from stick to slip and *vice versa*, the tangential stress vector $\boldsymbol{p_\tau}(\boldsymbol{x}, t)$ is supposed to be a continuous function of the coordinate $\boldsymbol{x}$, implying a number of additional BCs other than that at the leading edge given by Eq. (4).

The general solution to Eqs. (3) must be derived depending on the specific assumed constitutive equations, that is, the relationships between the tangential deformation vector $\boldsymbol{u_\tau}(\boldsymbol{x}, t)$ and the stresses $\boldsymbol{p_\tau}(\boldsymbol{x}, t)$. In turn, integrating the stresses over the contact patch $\mathscr{C}$ yields the global equilibrium equations

$$\boldsymbol{F_\tau}(t) = \iint_{\mathscr{C}} \boldsymbol{p_\tau}(\boldsymbol{x}, t)\, \mathrm{d}\boldsymbol{x}, \tag{9a}$$

$$M_z(t) = \iint_{\mathscr{C}} x p_y(\boldsymbol{x}, t) - y p_x(\boldsymbol{x}, t)\, \mathrm{d}\boldsymbol{x}. \tag{9b}$$

In steady-state, when the partial derivative $\partial \boldsymbol{u_\tau}(\boldsymbol{x}, t)/\partial t$ vanishes or may be neglected, Eqs. (3) provide a set of relationships between the tangential forces and moment acting in the contact patch and the creepage variables in the form

$$\boldsymbol{F_\tau}(\boldsymbol{\xi}, \phi) = \iint_{\mathscr{C}} \boldsymbol{p_\tau}(\boldsymbol{x}; \boldsymbol{\xi}, \phi)\, \mathrm{d}\boldsymbol{x}, \tag{10a}$$

$$M_z(\boldsymbol{\xi}, \phi) = \iint_{\mathscr{C}} x p_y(\boldsymbol{x}; \boldsymbol{\xi}, \phi) - y p_x(\boldsymbol{x}; \boldsymbol{\xi}, \phi)\, \mathrm{d}\boldsymbol{x}. \tag{10b}$$

3 Kalker's exact theory

The exact model developed by Kalker relies on the complete theory of elasticity [4], which prescribes the following constitutive relationship:

$$\boldsymbol{u}(\boldsymbol{x}, t) = \iint_{\mathscr{C}} \mathbf{A}(\boldsymbol{x}, \boldsymbol{x}') \boldsymbol{p}(\boldsymbol{x}', t)\, \mathrm{d}\boldsymbol{x}' + \boldsymbol{c}(t), \tag{11}$$

where $\boldsymbol{u}(\boldsymbol{x}, t) = [\boldsymbol{u_\tau}^{\mathrm{T}}(\boldsymbol{x}, t)\, u_z(\boldsymbol{x}, t)]^{\mathrm{T}}$ and $\boldsymbol{p}(\boldsymbol{x}, t) = [\boldsymbol{p_\tau}^{\mathrm{T}}(\boldsymbol{x}, t)\, p_z(\boldsymbol{x})]^{\mathrm{T}}$ are the deformation and stress vectors, $\mathbf{A}(\boldsymbol{x}, \boldsymbol{x}')$ is the *influence matrix*, and $\boldsymbol{c}(t)$ is a possibly time-varying vector of rigid displacements.

The integral convolution term in Eq. (11) poses unsurmountable difficulties in the derivation of a general analytical solution in transient conditions. In fact, the analysis of the transient problem within the theoretical framework of Kalker's exact model is limited to the case of pure longitudinal creepage and line contact, that is $\mathscr{C} = \{x \in \mathbb{R} \mid -a \le x \le a\}$. For the sake of simplicity, the contact patch and the vertical pressure distribution $p_z(x)$ are assumed to be fixed in the following investigation, but the more general case of time-varying contact length may be attacked using numerical methods or minimum principles [52, 53]. Owing to premises above, it is indeed possible to express the longitudinal deformation $u_x(x, t)$ as a sole function of the stress $p_x(x, t)$, since the influence matrix $\mathbf{A}(\boldsymbol{x}, \boldsymbol{x}')$ appearing in Eq. (11) becomes diagonal. Accordingly, the following scalar relationship may be derived:

$$u_x(x, t) = k F_x(t) - \frac{2(1-\nu)}{\pi G} \int_{-a}^{a} p_x(x', t) \ln|x' - x|\, \mathrm{d}x', \tag{12}$$

being k a constant determined by the geometry of the bodies, ν the Poisson's ratio, and G the modulus of rigidity. The relationship between the vertical deformation $u_z(t)$ and the pressure distribution $p_z(t)$ has a similar structure, with $p_z(t)$ given by the theory of Hertz [54, 55].

Moreover, the mathematical treatment of the problem may be simplified by introducing a new time-like variable, referred to as *travelled distance* and defined as $q \triangleq \int_0^t V(t')\, \mathrm{d}t'$. The additional assumption $V(t) > 0$ for all t implies that the mapping $t \mapsto q$ is one-to-one, and the transient rolling problem becomes actually independent of the rolling speed $V(t)$. More generally, when dealing with vector-valued rolling

velocity as in Eq. (1), it is possible to define $\bar{\boldsymbol{v}}_{\boldsymbol{\tau}}(\boldsymbol{x},t) = [\bar{v}_x(\boldsymbol{x},t) \; \bar{v}_y(\boldsymbol{x},t)]^{\mathrm{T}} \triangleq \boldsymbol{v}_{\boldsymbol{\tau}}/V(t)$ and consider nondimensional velocities. Replacing the time t with the travelled distance q, the longitudinal component of the governing PDEs in Eq. (3) may be more conveniently recast as

$$s_x(x,q) = \xi_x(q) + \frac{\partial u_x(x,q)}{\partial q} - \frac{\partial u_x(x,q)}{\partial x}, \qquad (x,q) \in (-a,a) \times \mathbb{R}_{>0}, \qquad (13)$$

subjected to the scalar version of the BC and IC (4) and (5), respectively, plus additional BCs enforcing the continuity in the transition from stick to slip and *vice versa*.

Substituting Eq. (12) (again with q in place of t) into (13) and integrating by parts yields [6]

$$s_x(x,q) = \xi_x(q) - k\frac{\mathrm{d}F_x(q)}{\mathrm{d}q} + \frac{2(1-\nu)}{\pi G} \int_{-a}^{a} \left(\frac{\partial p_x(x',q)}{\partial q} - \frac{\partial p_x(x',q)}{\partial x'} \right) \ln|x'-x| \, \mathrm{d}x', \qquad (14)$$
$$(x,q) \in (-a,a) \times \mathbb{R}_{>0},$$

since $p_x(-a,q) = p_x(a,q) = 0$ for all q. According to Eq. (14), the solution to the transient rolling contact problem has been reduced to the determination of the difference between the partial derivatives of the longitudinal shear stress $p_x(x',q)$ in the integral term. To this end, in any stick zone $\mathscr{C}^{(\mathrm{a})}$, Eq. (14) may be differentiated with respect to the space coordinate x yielding

$$\frac{\partial s_x(x,q)}{\partial x} = -\frac{2(1-\nu)}{\pi G} \int_{-a}^{a} \left(\frac{\partial p_x(x',q)}{\partial q} - \frac{\partial p_x(x',q)}{\partial x'} \right) \frac{\mathrm{d}x'}{x'-x}, \qquad (x,q) \in \mathscr{\mathring{C}}^{(\mathrm{a})} \times \mathbb{R}_{>0}, \qquad (15)$$

whilst in any slip zone $\mathscr{C}^{(\mathrm{s})}$, recalling that the vertical pressure distribution is assumed to be independent of q, the following equation may be derived:

$$\frac{\partial p_x(x,q)}{\partial q} - \frac{\partial p_x(x,q)}{\partial x} = \pm\frac{\mathrm{d}p_z(x)}{\mathrm{d}x} = \mp p_z^* \frac{x}{\sqrt{1-x^2}}, \qquad (x,q) \in \mathscr{\mathring{C}}^{(\mathrm{s})} \times \mathbb{R}_{>0}, \qquad (16)$$

where the sign must be correctly determined so as to ensure the continuity of the solution in the transition between stick to slip conditions.

The Hilbert problem described by Eqs. (15) and (16) admits a unique solution adding the closure relationship

$$\frac{\mathrm{d}F_x(q)}{\mathrm{d}q} = \int_{-a}^{a} \frac{\partial p_x(x,q)}{\partial q} - \frac{\partial p_x(x,q)}{\partial x} \, \mathrm{d}x, \qquad (17)$$

which prescribes the global equilibrium, owing again to the identity $p_x(-a,q) = p_x(a,q) = 0$. The calculation of the solution is then incremental and may be carried out by using numerical techniques [6]. The trend of the shear stresses converges systematically to the steady-state solution derived by Carter [40], approximately after travelling a distance $q = 2a$. The transient evolution of the longitudinal shear stress for a wheel-rail system subjected to a constant longitudinal creepage, starting from Cattaneo's initial conditions, is illustrated, for example, in the books by Kalker [7] and Johnson [8].

4 Kalker's simplified theory

Even in the steady-state case, the exact formulation developed by Kalker, based on the complete theory of elasticity, is computationally costly. Moreover, its intrinsic complexity restricts the transient analysis to the case of pure longitudinal creepage. In his simplified theory [17], Kalker replaced the original relationship between the deformation vector $\boldsymbol{u}_{\boldsymbol{\tau}}(\boldsymbol{x},t)$ and the tangential shear stresses $\boldsymbol{p}_{\boldsymbol{\tau}}(\boldsymbol{x},t)$ with that of a linear elastic foundation (a similar approximation is also used in road vehicle dynamics). In vector notation, the constitutive equations are therefore postulated in the form

$$\boldsymbol{u}_{\boldsymbol{\tau}}(\boldsymbol{x},t) = \mathbf{L}_{\boldsymbol{\tau}} \boldsymbol{p}_{\boldsymbol{\tau}}(\boldsymbol{x},t), \qquad (18)$$

being the *flexibility matrix* $\mathbf{L}_{\boldsymbol{\tau}}$ a positive definite matrix, often assumed to be diagonal, as also done in the present paper, i.e.,

$$\mathbf{L}_{\boldsymbol{\tau}} = \begin{bmatrix} L_x & 0 \\ 0 & L_y \end{bmatrix}, \qquad (19)$$

usually with $L_x = L_y = L$. In this paper, the generalisation to a matrix of flexibilities, rather than a single value, is inspired by some recent results presented in [56].

Since the flexibility matrix $\mathbf{L_\tau}$ is nonsingular, according to Kalker's simplified theory, the original BC (4) and IC (5) may be more conveniently enforced concerning the deformations rather than the shear stresses, yielding a system of linear transport equations, that is, linear hyperbolic PDEs. Furthermore, no-slip conditions, corresponding approximately to infinite friction inside the contact patch (i.e., $\mu \to \infty$) or to sufficiently small creepages, may be analysed easily by setting $\boldsymbol{s}(\boldsymbol{x}, t) = \mathbf{0}$ for all $\boldsymbol{x} \in \mathscr{C}$, that is, $\mathscr{C}^{(\mathrm{a})} \equiv \mathscr{C}$. This has the additional advantage that, in many cases, the corresponding solution in the slip region may be easily recovered by constraining the transient stresses calculated in no-slip conditions below the traction bound.

4.1 No-slip conditions

Replacing again the time variable t with the travelled distance q, under no-slip assumptions, the governing PDEs of the model may be restated as

$$\frac{\partial \boldsymbol{u_\tau}(\boldsymbol{x}, q)}{\partial q} + \bar{\boldsymbol{v}}_{\boldsymbol{\tau}}(\boldsymbol{x}, q) \cdot \nabla_{\boldsymbol{\tau}} \boldsymbol{u_\tau}(\boldsymbol{x}, q) = -\boldsymbol{\xi}(q) - \mathbf{A}_\phi(q)\boldsymbol{x}, \qquad (\boldsymbol{x}, q) \in \mathscr{\mathring{C}} \times \mathbb{R}_{>0}, \qquad (20)$$

or, considering explicitly $\bar{\boldsymbol{v}}_{\boldsymbol{\tau}}(\boldsymbol{x}, q) = -\hat{\boldsymbol{e}}_x$,

$$\frac{\partial \boldsymbol{u_\tau}(\boldsymbol{x}, q)}{\partial q} - \frac{\partial \boldsymbol{u_\tau}(\boldsymbol{x}, q)}{\partial x} = -\boldsymbol{\xi}(q) - \mathbf{A}_\phi(q)\boldsymbol{x}, \qquad (\boldsymbol{x}, q) \in \mathscr{\mathring{C}} \times \mathbb{R}_{>0}. \qquad (21)$$

Both Eqs. (20) and (21) come equipped with the following BC and IC for the transient deformation:

BC: $\qquad \boldsymbol{u_\tau}(\boldsymbol{x}, q) = \mathbf{0}, \qquad (\boldsymbol{x}, q) \in \mathscr{L} \times \mathbb{R}_{>0}, \qquad (22)$

IC: $\qquad \boldsymbol{u_\tau}(\boldsymbol{x}, 0) = \boldsymbol{u}_{\boldsymbol{\tau}0}(\boldsymbol{x}), \qquad \boldsymbol{x} \in \mathscr{\mathring{C}}_0. \qquad (23)$

It may be also observed that, in this case, it is convenient to replace the original notions of leading, neutral and trailing edges with

$$\mathscr{L} \triangleq \left\{ \boldsymbol{x} \in \partial\mathscr{C} \; \middle| \; \left[\bar{\boldsymbol{v}}_{\boldsymbol{\tau}}(\boldsymbol{x}, q) - \bar{\boldsymbol{v}}_{\partial\mathscr{C}}(\boldsymbol{x}, q) \right] \cdot \hat{\boldsymbol{n}}_{\partial\mathscr{C}}(\boldsymbol{x}, q) < 0 \right\}, \qquad (24\mathrm{a})$$

$$\mathscr{N} \triangleq \left\{ \boldsymbol{x} \in \partial\mathscr{C} \; \middle| \; \left[\bar{\boldsymbol{v}}_{\boldsymbol{\tau}}(\boldsymbol{x}, q) - \bar{\boldsymbol{v}}_{\partial\mathscr{C}}(\boldsymbol{x}, q) \right] \cdot \hat{\boldsymbol{n}}_{\partial\mathscr{C}}(\boldsymbol{x}, q) = 0 \right\}, \qquad (24\mathrm{b})$$

$$\mathscr{T} \triangleq \left\{ \boldsymbol{x} \in \partial\mathscr{C} \; \middle| \; \left[\bar{\boldsymbol{v}}_{\boldsymbol{\tau}}(\boldsymbol{x}, q) - \bar{\boldsymbol{v}}_{\partial\mathscr{C}}(\boldsymbol{x}, q) \right] \cdot \hat{\boldsymbol{n}}_{\partial\mathscr{C}}(\boldsymbol{x}, q) > 0 \right\}, \qquad (24\mathrm{c})$$

where $\bar{\boldsymbol{v}}_{\partial\mathscr{C}}(\boldsymbol{x}, q)$ denotes the corresponding nondimensional velocity of the boundary of the contact patch. It is worth remarking once again that $\bar{\boldsymbol{v}}_{\partial\mathscr{C}}(\boldsymbol{x}, q) = \mathbf{0}$ in the case of a fixed contact patch, i.e., $\mathscr{C}(q) \equiv \mathscr{C}_0$. As formally defined in Eq. (24a), the notion of leading edge ensures once again the BC (22) to be noncharacteristic.

The solution to the above Eqs. (21) may be sought resorting to the method of the characteristic lines for hyperbolic PDEs [43–45], and depends on the initial datum encountered when imposing the BC (22) and the IC (23), in turn. In particular, considering a fixed contact patch $\mathscr{C}(q) \equiv \mathscr{C}_0$, it is possible to define the vector-valued function $\boldsymbol{u}_{\boldsymbol{\tau}}^-(\boldsymbol{x}, q) = [u_x^-(\boldsymbol{x}, q) \; u_y^-(\boldsymbol{x}, q)]^{\mathrm{T}}$ as

$$\boldsymbol{u}_{\boldsymbol{\tau}}^-(\boldsymbol{x}, q) = -\int_x^{x_{\mathscr{L}}(y)} \left(\boldsymbol{\xi}(x - x' + q) + \mathbf{A}_\phi(x - x' + q) \begin{bmatrix} x' \\ y \end{bmatrix} \right) \mathrm{d}x', \qquad (\boldsymbol{x}, q) \in \mathscr{C}^- \times \mathbb{R}_{\geq 0}, \qquad (25)$$

and analogously $\boldsymbol{u}_{\boldsymbol{\tau}}^+(\boldsymbol{x}, q) = [u_x^+(\boldsymbol{x}, q) \; u_y^+(\boldsymbol{x}, q)]^{\mathrm{T}}$ as

$$\boldsymbol{u}_{\boldsymbol{\tau}}^+(\boldsymbol{x}, q) = -\int_0^q \left(\boldsymbol{\xi}(q') + \mathbf{A}_\phi\phi(q') \begin{bmatrix} x + q - q' \\ y \end{bmatrix} \right) \mathrm{d}q' + \boldsymbol{u}_{\boldsymbol{\tau}0}(x + q, y), \qquad (\boldsymbol{x}, q) \in \mathscr{C}^+ \times \mathbb{R}_{\geq 0}, \qquad (26)$$

where $x_{\mathscr{L}}(y)$ denotes an explicit parametrisation of the leading edge[3]. The analytical expressions derived in Eqs. (25) and (26) correspond to the prescription of the BC (22) and IC (23), respectively. In the simplified theory, indeed, at least in no-slip conditions, it is always possible to determine where, inside

---

[3]For example, for an elliptical contact patch $x_{\mathscr{L}}(y) = a\sqrt{1 - (y/b)^2}$.

the contact patch, transient and stationary effects are taking place. In fact, the separation between the transient and stationary regions of the contact patch solely depends on the structure of the governing PDEs (21). Accordingly, in vector notation, the global solution may be constructed as

$$\boldsymbol{u}_{\boldsymbol{\tau}}(\boldsymbol{x}, q) = \begin{cases} \boldsymbol{u}_{\boldsymbol{\tau}}^-(\boldsymbol{x}, q), & (\boldsymbol{x}, q) \in \mathscr{C}^- \times \mathbb{R}_{\geq 0}, \\ \boldsymbol{u}_{\boldsymbol{\tau}}^+(\boldsymbol{x}, q), & (\boldsymbol{x}, q) \in \mathscr{C}^+ \times \mathbb{R}_{\geq 0}, \end{cases} \tag{27}$$

where, as anticipated above, $\mathscr{C}^- \triangleq \{\boldsymbol{x} \in \mathscr{C} \mid x_{\mathscr{L}}(y) - q < x \leq x_{\mathscr{L}}(y)\}$ and $\mathscr{C}^+ \triangleq \{\boldsymbol{x} \in \mathscr{C} \mid -x_{\mathscr{L}}(y) \leq x \leq x_{\mathscr{L}}(y) - q\}$ denote the stationary and transient regions of the contact patch. It should be noticed that $\mathscr{C} = \mathscr{C}^- \cup \mathscr{C}^+$. Moreover, if the contact patch is D-convex in the rolling direction according to the following Assumption 4.1, the natural requirement $\boldsymbol{u}_{\boldsymbol{\tau} 0}(x_{\mathscr{L}}(y), y) = \boldsymbol{0}$ additionally ensures that $\boldsymbol{u}_{\boldsymbol{\tau}} \in C^0(\mathscr{C} \times \mathbb{R}_{\geq 0}; \mathbb{R}^2)$ for any combination of creepages $(\boldsymbol{\xi}, \phi) \in C^0(\mathbb{R}_{\geq 0}; \mathbb{R}^3)$ and initial conditions $\boldsymbol{u}_{\boldsymbol{\tau} 0} \in C^0(\mathscr{C}; \mathbb{R}^2)$ [34]. On the other hand, C^1 regularity (that is, the existence of continuously differentiable solutions) is not guaranteed automatically, since the deformations $\boldsymbol{u}_{\boldsymbol{\tau}}^-(\boldsymbol{x}, q)$ and $\boldsymbol{u}_{\boldsymbol{\tau}}^+(\boldsymbol{x}, q)$ are only continuous for $x = x_{\mathscr{L}}(y) - q$, as it usually happens in transport phenomena.

More generally, the theory presented so far is well-posed in the sense of weak solutions. For example, if the contact patch is fixed, has Lipschitz boundary and the nondimensional rolling velocity $\bar{\boldsymbol{v}}_{\boldsymbol{\tau}}(\boldsymbol{x}, q)$ is sufficiently regular, the existence and uniqueness of a generalised or weak solution $\boldsymbol{u}_{\boldsymbol{\tau}}(\boldsymbol{x}, q) \in L^\infty(\mathring{\mathscr{C}} \times (0, Q); \mathbb{R}^2)$ to the problem described by Eqs. (20), (22) and (23) are guaranteed under very mild assumptions in any interval $q \in (0, Q)$ [57, 58]. Alternatively, more restrictive assumptions also allow treating the problem, even in presence of time-varying contact patch, as in [59]. In any case, the formulae given in Eqs. (25) and (26) considerably simplify when the creepages are constant over travelled distance:

$$\boldsymbol{u}_{\boldsymbol{\tau}}^-(\boldsymbol{x}) = -\boldsymbol{\xi}\big(x_{\mathscr{L}}(y) - x\big) - \mathbf{A}_\phi\big(x_{\mathscr{L}}(y) - x\big) \begin{bmatrix} (x_{\mathscr{L}}(y) + x)/2 \\ y \end{bmatrix}, \qquad (\boldsymbol{x}, q) \in \mathscr{C}^- \times \mathbb{R}_{\geq 0}, \tag{28}$$

and

$$\boldsymbol{u}_{\boldsymbol{\tau}}^+(\boldsymbol{x}, q) = -\boldsymbol{\xi} q - \mathbf{A}_\phi q \begin{bmatrix} x + q/2 \\ y \end{bmatrix} + \boldsymbol{u}_{\boldsymbol{\tau} 0}(x + q, y), \qquad (\boldsymbol{x}, q) \in \mathscr{C}^+ \times \mathbb{R}_{\geq 0}. \tag{29}$$

In particular, it may be noticed that the stationary solution $\boldsymbol{u}_{\boldsymbol{\tau}}^-(\boldsymbol{x})$ becomes independent of q, and moreover coincides with the steady-state deformation obtained when all the involved quantities are constant over time or, equivalently, travelled distance. In fact, in this case the solution $\boldsymbol{u}_{\boldsymbol{\tau}}^-(\boldsymbol{x})$ is not only stationary, but also steady-state. Moreover, since the steady-state solution is defined for $x > x_{\mathscr{L}}(y) - q$, it becomes clear that, in no-slip conditions, any transient extinguishes exactly after travelling a distance $q = 2a$, being a the semilength of the contact patch (for en elliptical geometry, it also coincides with the semiaxis). This is also in accordance with what predicted by the exact solution proposed by Kalker based on the theory of elasticity.

4.2 Partial slip conditions

In case of limited friction, the adhesion solutions given by Eqs. (25) and (26) (or (21) and (20)) are again valid until the magnitude of the tangential shear stress $\boldsymbol{p}_{\boldsymbol{\tau}}(\boldsymbol{x}, q)$ acting at the coordinate $\boldsymbol{x}$ is below the corresponding value of the traction bound $\mu p_z(\boldsymbol{x})$. According to the simplified theory, the deformation in the slip region $\mathscr{C}^{(\mathrm{s})}$ may be then calculated as

$$\boldsymbol{u}_{\boldsymbol{\tau}}^{(\mathrm{s})}(\boldsymbol{x}, q) = -\mathbf{L}_{\boldsymbol{\tau}} \mu p_z(\boldsymbol{x}) \frac{\boldsymbol{s}(\boldsymbol{x}, q)}{s(\boldsymbol{x}, q)} \iff s(\boldsymbol{x}, q) \neq 0, \tag{30}$$

and may generally be time-varying. On the other hand, the deformation $\boldsymbol{u}_{\boldsymbol{\tau}}^{(\mathrm{a})}(\boldsymbol{x}, q)$ in the adhesion zone $\mathscr{C}^{(\mathrm{a})}$ may obtained combining Eqs. Eqs. (25), (26) (or alternatively (21) and (20) when the creepages are constant) with (27). The corresponding shear stress are denoted in the following by $\boldsymbol{p}_{\boldsymbol{\tau}}^{(\mathrm{a})}(\boldsymbol{x}, q) = \mathbf{L}_{\boldsymbol{\tau}}^{-1} \boldsymbol{u}_{\boldsymbol{\tau}}^{(\mathrm{a})}(\boldsymbol{x}, q)$ and $\boldsymbol{p}_{\boldsymbol{\tau}}^{(\mathrm{s})}(\boldsymbol{x}, q) = \mathbf{L}_{\boldsymbol{\tau}}^{-1} \boldsymbol{u}_{\boldsymbol{\tau}}^{(\mathrm{s})}(\boldsymbol{x}, q)$, respectively.

A major complication connected with partial slip occurring inside the contact patch, however, is that the analytical solutions in the slip zone cannot be recovered in the most general case of combined creepage and spin conditions. In particular, owing to the additional condition $L_x = L_y = L$, closed-form solutions are restricted to the case of constant creepages. As already mentioned, assuming a parabolic pressure distribution and sufficiently small spin, the transient solutions may still be constructed by constraining

the expressions derived in Eqs. (21) and (20) below the traction bound [34]. In case of limited friction, smaller distance need generally to be travelled to reach steady-state conditions, at least if the spin slip vanishes. In this paper, the problem is treated limitedly to the case of pure longitudinal creepage, for which any general concave or strictly concave pressure distribution may be considered, according to the already-mentioned Assumption 4.1. Concerning the simpler situation of line contact, a similar analysis may however be conducted to take also into account the effect of small spin creepages, as done, e.g., in [34] adopting a different sign convention.

Assumption 4.1. *The contact patch $\mathscr{C}$ is a compact, D-convex[4] set along the direction $\hat{\boldsymbol{e}}_x$. Moreover, for every $\boldsymbol{x} \in \mathscr{C}$, consider the restrictions of the contact patch and vertical pressure distribution obtained for y fixed, i.e., $\mathscr{C}^{(y)} \triangleq \mathscr{C} \!\restriction_y$ and $p_z^{(y)}(x) \triangleq p_z(\boldsymbol{x}) \!\restriction_y$. It is assumed that $p_z^{(y)} \in C^1(\mathscr{C}^{(y)}; \mathbb{R})$, with $p_z^{(y)}(x) = 0$ on $\partial \mathscr{C}^{(y)}$ and $p_z^{(y)}(\cdot)$ strictly concave (i.e., $p_z(\cdot)$ strictly D-concave in direction $\hat{\boldsymbol{e}}_x$).*

Owing to the previous Assumption 4.1, and considering ICs satisfying $u_{y0}(\boldsymbol{\xi}) = 0$, the following two Lemmata (analogous to those proved in [34]) may be easily established, which generalise the findings of Kalker's [61] and have a clear physical meaning.

Lemma 4.1. *Consider pure longitudinal creepage conditions, i.e., $\xi_x \neq 0$, $\xi_y = 0$, $\phi = 0$. Then, if $p_z(\boldsymbol{x})$ satisfies Assumption 4.1 and $L|p_{x0}(\boldsymbol{x})| = |u_{x0}(\boldsymbol{x})| \leq \mu p_z(\boldsymbol{x})$ for all $\boldsymbol{x} \in \mathscr{C}$, the following implications hold for all $(\boldsymbol{x}, q) \in \mathscr{C} \times \mathbb{R}_{>0}$ such that $x \in [-x_{\mathscr{L}}(y), x_{\mathscr{L}}(y))$:*

$$\xi_x \geq 0 \qquad \Longrightarrow \qquad p_x^{(\mathrm{a})}(\boldsymbol{x}, q) > -\mu p_z(\boldsymbol{x}), \qquad |\xi_x| \leq -\mu L \frac{\partial p_z(\boldsymbol{x})}{\partial x}, \qquad (31\mathrm{a})$$

$$\xi_x \geq 0 \qquad \Longrightarrow \qquad p_x^{(\mathrm{a})}(\boldsymbol{x}, q) < \mu p_z(\boldsymbol{x}), \qquad |\xi_x| \geq \mu L \frac{\partial p_z(\boldsymbol{x})}{\partial x}, \qquad (31\mathrm{b})$$

$$\xi_x < 0 \qquad \Longrightarrow \qquad p_x^{(\mathrm{a})}(\boldsymbol{x}, q) < \mu p_z(\boldsymbol{x}), \qquad |\xi_x| \leq -\mu L \frac{\partial p_z(\boldsymbol{x})}{\partial x}, \qquad (31\mathrm{c})$$

$$\xi_x < 0 \qquad \Longrightarrow \qquad p_x^{(\mathrm{a})}(\boldsymbol{x}, q) > -\mu p_z(\boldsymbol{x}), \qquad |\xi_x| \geq \mu L \frac{\partial p_z(\boldsymbol{x})}{\partial x}. \qquad (31\mathrm{d})$$

Proof. The proofs for $\xi_x \geq 0$ and $\xi_x < 0$ are mirrored, and thus only the analysis for $\xi_x \geq 0$ is conducted.

1. Consider the case $\xi_x \geq 0, |\xi_x| \leq -\mu L \dfrac{\partial p_z(\boldsymbol{x})}{\partial x}$. For $x \in (x_{\mathscr{L}}(y) - q, x_{\mathscr{L}}(y))$, Eq. (21) gives

$$p_x^{(\mathrm{a})}(\boldsymbol{x}, q) = p_x^-(\boldsymbol{x}) = -\frac{1}{L}|\xi_x|\left(x_{\mathscr{L}}(y) - x\right) \geq \mu \frac{\partial p_z(\boldsymbol{x})}{\partial x}\left(x_{\mathscr{L}}(y) - x\right) > -\mu p_z(\boldsymbol{x}), \qquad (32)$$

where the last inequality follows from Assumption 4.1. For $x \in [-x_{\mathscr{L}}(y), x_{\mathscr{L}}(y) - q]$, from Eq. (20):

$$p_x^{(\mathrm{a})}(\boldsymbol{x}, q) = p_x^+(\boldsymbol{x}, q) = -\frac{1}{L}|\xi_x| q + \frac{1}{L}u_{x0}(x + q, y) \geq \mu \frac{\partial p_z(\boldsymbol{x})}{\partial x} q - \mu p_z(x + q, y) > -\mu p_z(\boldsymbol{x}), \quad (33)$$

the last inequality following from Assumption 4.1. Combining (32) and (33), (31a) is deduced.

2. Consider the case $\xi_x \geq 0, |\xi_x| \geq \mu L \dfrac{\partial p_z(\boldsymbol{x})}{\partial x}$. For $x \in (x_{\mathscr{L}}(y) - q, x_{\mathscr{L}}(y))$, Eq. (21) gives

$$p_x^{(\mathrm{a})}(\boldsymbol{x}, q) = p_x^-(\boldsymbol{\xi}) = -\frac{1}{L}|\xi_x|\left(x_{\mathscr{L}}(y) - x\right) \leq -\mu \frac{\partial p_z(\boldsymbol{x})}{\partial x}\left(x_{\mathscr{L}}(y) - x\right) < \mu p_z(\boldsymbol{x}). \qquad (34)$$

For $x \in [-x_{\mathscr{L}}(y), x_{\mathscr{L}}(y) - q]$, from Eq. (20):

$$p_x^{(\mathrm{a})}(\boldsymbol{x}, q) = p_x^+(\boldsymbol{x}, q) = -\frac{1}{L}|\xi_x| q + \frac{1}{L}u_{x0}(x + q, y) \leq -\mu \frac{\partial p_z(\boldsymbol{x})}{\partial x} q + \mu p_z(x + q, y) < \mu p_z(\boldsymbol{x}), \quad (35)$$

the last inequality following from Assumption 4.1. Combining (34) and (35), (31b) is deduced.

$\square$

---

[4]A D-convex set is a set convex along a specified direction. Analogously, a D-convex function is a function that is convex along a given direction. The reader may refer to [60] for additional details.

Lemma 4.2. *Consider pure longitudinal creepage conditions, i.e., $\xi_x \neq 0$, $\xi_y = 0$, $\phi = 0$, and a vertical pressure distribution $p_z(\boldsymbol{x})$ satisfying Assumption 4.1. Then, the following implications hold for all $(\boldsymbol{x}, q) \in \mathscr{P} \times \mathbb{R}_{>0}$ such that $(x - \delta q, \delta q) \in [-x_{\mathscr{L}}(y), x_{\mathscr{L}}(y)) \times \mathbb{R}_{>0}$:*

$$\xi_x \geq 0, \, p_x^{(\mathrm{a})}(\boldsymbol{x}, q) \geq \mu p_z(\boldsymbol{x}) \quad \Longrightarrow \quad p_x^{(\mathrm{a})}(x - \delta q, y, q + \delta q) > \mu p_z(x - \delta q, y), \quad \text{(36a)}$$

$$\xi_x \geq 0, \, p_x^{(\mathrm{a})}(\boldsymbol{\xi}, q) \leq -\mu p_z(\boldsymbol{\xi}) \quad \Longrightarrow \quad p_x^{(\mathrm{a})}(x - \delta q, y, q + \delta q) < -\mu p_z(x - \delta q, y), \quad \text{(36b)}$$

$$\xi_x < 0, \, p_x^{(\mathrm{a})}(\boldsymbol{\xi}, q) \geq \mu p_z(\boldsymbol{\xi}) \quad \Longrightarrow \quad p_x^{(\mathrm{a})}(x - \delta q, y, q + \delta q) > \mu p_z(x - \delta q, y), \quad \text{(36c)}$$

$$\xi_x < 0, \, p_x^{(\mathrm{a})}(\boldsymbol{\xi}, q) \leq -\mu p_z(\boldsymbol{\xi}) \quad \Longrightarrow \quad p_x^{(\mathrm{a})}(x - \delta q, y, q + \delta q) < -\mu p_z(x - \delta q, y). \quad \text{(36d)}$$

Proof. Again, the Lemma is only proved for $\xi_x \geq 0$; the cases for $\xi_x < 0$ are specular.

1. Consider the case $\xi_x \geq 0, p_x^{(\mathrm{a})}(\boldsymbol{x}, q) \geq \mu p_x(\boldsymbol{x})$. First it is observed that, owing to (31a), it must necessarily be $|\xi_x| < \mu L \dfrac{\partial p_z(\boldsymbol{x})}{\partial x}$ to have $p_z^{(\mathrm{a})}(\boldsymbol{x}, q) \geq \mu p_z(\boldsymbol{x})$. Thus, recalling Assumption 4.1 and Eqs. (21) and (20), it holds that

$$p_x^{(\mathrm{a})}(x - \delta q, y, q + \delta q) = -\frac{1}{L} |\xi_x| \, \delta q + p_x^{(\mathrm{a})}(\boldsymbol{x}, q) > -\mu \frac{\partial p_z(\boldsymbol{x})}{\partial x} \delta q + \mu p_z(\boldsymbol{x}) > \mu p_z(x - \delta q, y). \quad \text{(37)}$$

2. Consider the case $\xi_x \geq 0, p_x^{(\mathrm{a})}(\boldsymbol{x}, q) \leq -\mu p_z(\boldsymbol{x})$. First it is observed that, owing to (31b), it must necessarily be $|\xi_x| > -\mu \dfrac{\partial p_z(\boldsymbol{x})}{\partial x}$ to have $p_x^{(\mathrm{a})}(\boldsymbol{x}, q) \leq -\mu p_z(\boldsymbol{x})$. Thus, recalling Assumption 4.1 and Eqs. (21) and (20), it holds that

$$p_x^{(\mathrm{a})}(x - \delta q, y, q + \delta q) = -\frac{1}{L} |\xi_x| \, \delta q + p_x^{(\mathrm{a})}(\boldsymbol{x}, q) < \mu \frac{\partial p_z(\boldsymbol{x})}{\partial x} \delta q - \mu p_z(\boldsymbol{x}) < -\mu p_z(x - \delta q, y). \quad \text{(38)}$$

$\square$

It is worth pointing out that, more generally, if Assumption 4.1 is only satisfied with $p_z^{(y)}(\cdot)$ concave but not strictly concave, the right-hand sides of implications (31) hold non-strictly for all $(\boldsymbol{x}, q) \in \mathscr{C} \times \mathbb{R}_{>0}$. Also, the right-hand sides of implications (36) hold non-strictly. Additionally, if Assumption 4.1 is only satisfied with $p_z^{(y)} \in C^1(\mathring{\mathscr{C}}^{(y)}; \mathbb{R})$ for some or every fixed y, then, for those fixed y, the results advocated in Lemma 4.1 are only valid for $(x, q) \in \mathring{\mathscr{C}}^{(y)} \times \mathbb{R}_{>0}$. The same holds if $p_z^{(y)}(\cdot)$ in Assumption 4.1 is concave but not strictly concave.

The physical interpretation of Lemmata 4.1 and 4.2 is as follows. Lemma 4.1 asserts that the slip solutions calculated by constraining the adhesion shear stresses below the traction bound are always valid. This is ensured by the fact that the relative slip does not vanish whenever the adhesion solution exceeds the traction bound in absolute value. On the other hand, Lemma 4.2 formalises mathematically the fact that, once a material point starts slipping, it continues doing so until it relinquishes the contact patch. This result should be understood concerning the Lagrangian approach: a particle that occupies the longitudinal position x at travelled distance q will be located at $x - \delta q$ at time $q + \delta q$, being the lateral coordinate clearly unchanged.

For a fair comparison with the exact solution found by Kalker, Fig. 1 shows again the transient trend of the shear stress $p_x(\boldsymbol{x}, q)$ for a railway wheel subjected to a pure, constant longitudinal creepage ξ_x, starting from initial conditions corresponding to Cattaneo's distribution (in the equivalent framework of the simplified theory).

4.3 Time-varying contact patch

Finally, the case of time-varying contact patch $\mathscr{C} = \mathscr{C}(t)$ may be of interest when investigating dissipation and instability effects connected with corrugation phenomena, as done for example in a relatively recent series of papers [22–24]. Whilst an analytical solution cannot be obtained in such a case, even concerning no-slip conditions, a possible technique to approach the problem consists in mapping the time-varying geometry of the contact patch into a fixed spatial domain by a suitable change of coordinates[5], yielding a system of uncoupled PDEs with a possibly vector-valued transport velocity of the same form as that in Eqs. (20). Continuing the discussion initiated in Sect. 4.1, limitedly to the situation of no-slip,

---

[5]This approach is particularly advantageous when it comes to apply numerical methods, such as FEMs and BEMs.
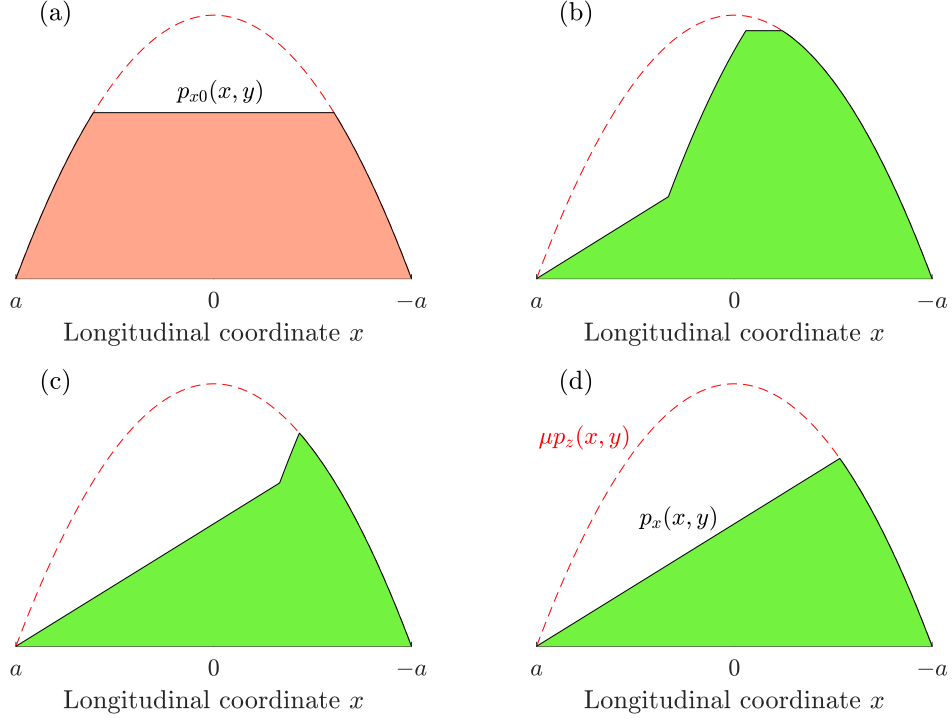
Figure 1: Transient evolution of the longitudinal shear stress $p_x(\boldsymbol{x}, q)$ due to a pure longitudinal creepage input ξ_x, starting from Cattaneo's initial conditions, according to Kalker's simplified theory. The figure refers to the middle plane of the contact patch ($x_{\mathscr{L}}(y) = x_{\mathscr{L}}(0) = a$). (a) $q = 0$; (b) $q = 2x_{\mathscr{L}}(y)/3$; (c) $q = 4x_{\mathscr{L}}(y)/3$; (d) $q = 2x_{\mathscr{L}}(y)$.

the existence and uniqueness of the solution follow then from similar arguments as in the case of fixed geometry (see Appendix A) [57, 58]. For example, restricting the attention to the longitudinal problem under the assumptions of line contact and pure longitudinal creepage, it is demonstrated in Appendix A that the original PDE in Eqs. (20) may be converted into the form

$$\frac{\partial \tilde{u}_x(\tilde{x}, \tilde{q})}{\partial \tilde{q}} - \frac{1}{a(\tilde{q})}\left(1 + \tilde{x}\,\frac{\partial a(\tilde{q})}{\partial \tilde{q}}\right)\frac{\partial \tilde{u}_x(\tilde{x}, \tilde{q})}{\partial \tilde{x}} = -\tilde{\xi}_x(\tilde{q}), \qquad (\tilde{x}, \tilde{q}) \in \mathring{\mathscr{C}} \times \mathbb{R}_{>0}, \qquad (39)$$

where $\tilde{x} \triangleq x/a(q)$, $\tilde{q} \equiv q$, $\tilde{u}_x(\tilde{x}, \tilde{q}) \triangleq u_x(a(q)\tilde{x}, \tilde{q})$, $\tilde{\xi}_x(\tilde{q}) \triangleq \xi_x(q)$, and $\mathscr{C} = \{x \in \mathbb{R} \mid -1 \leq x \leq 1\}$ (see Example A.1). The corresponding BC and IC may be deduced as

BC:	$\tilde{u}_x(1, \tilde{q}) = 0,$	$\tilde{q} \in \mathbb{R}_{>0},$	(40)
IC:	$\tilde{u}_x(\tilde{x}, 0) = \tilde{u}_{x0}(\tilde{x}) = u_{x0}\big(a(0)x\big),$	$x \in \mathring{\mathscr{C}}_0.$	(41)

If the function $a(\cdot)$ is sufficiently regular, the problem is well-posed and may even be attacked within standard mathematical frameworks [62, 63]. In particular, if $a(\tilde{q}) \in [a_{\min}, a_{\max}]$, with $a_{\min} > 0$, and $\left|\partial a(\tilde{q})/\partial \tilde{q}\right| < 1$ for all $q \in \mathbb{R}_{>0}$, the formulation described by Eq. (39) preserves the noncharacteristic property of the BC (40). As already mentioned, Eq. (39) does not generally admit a closed-form solution, and numerical methods are required. In this context, a detailed review of possible techniques is presented, e.g., in [63–65].

In any case, the time evolution of the deformations and shear stresses acting at the wheel-rail interface is similar to that illustrated in Fig. 1 for the situation of fixed contact patch, and omitted here for brevity. Instead, the formulation introduced according to Eqs. (39), (40) and (41) is used in Sect. 6.1.2 as a reference to validate a simplified, pragmatic transient model. Indeed, the time-varying forces and moment may be calculated directly with the aid of the formulae in Eqs. (101), as clarified in Appendix A.

5 Two-regime theory

For railway vehicle dynamics and control applications, it may be desirable to describe the transient rolling contact problem using simplified models formulated in terms od ordinary differential equations (ODEs) rather than PDEs. Such models may be conveniently derived from the steady-state formulae for the force-creepage laws already available from the literature, as shown in [31, 39]. Therefore, in this section, the *two-regime theory* originally developed in [39] is adapted to explain nonstationary effects concerning the wheel-rail interaction. As opposed to the exact and simplified theories discussed previously, the main advantage of the two-regime formulation resides in that it is entirely analytical, and only requires a reduced number of lumped states to capture unsteady phenomena. It is perhaps interesting to observe that the interpretation of the transient phenomenon within the framework of the two-regime models aligns with the perspective of *feeding* versus *leaking*, offered by Vollebregt in [66].

5.1 Motivating example

The fundamental idea behind the two-regime formulation is to approximate the governing PDEs (3) by two different systems of ODEs, and then interpolate between their solution to describe the transient evolution of the force-creepage characteristics. To illustrate the intuition behind the proposed approach, it may perhaps be beneficial to consider the case of pure longitudinal creepage in isolation, and analyse the transient behaviour within the framework of Kalker's simplified theory. Coming back to the original time variable t in place of the travelled distance q, and assuming no-slip conditions for the sake of simplicity, at very low rolling speed $V(t) \to 0$, the longitudinal equation in Eq. (3) may be approximated as

$$\frac{\partial u_x(\boldsymbol{x}, t)}{\partial t} - V(t) \frac{\partial u_x(\boldsymbol{x}, t)}{\partial x} \approx \frac{\partial u_x(\boldsymbol{x}, t)}{\partial t} = -V(t)\xi_x(t), \qquad (\boldsymbol{x}, t) \in \mathscr{C} \times \mathbb{R}_{>0}. \tag{42}$$

It should be observed that the term $-V(t)\xi_x(t)$ on the right-hand side of Eq. (42) does not vanish, since $V(t)$ cancels out with the denominator of $\xi_x(t)$. Dividing by the flexibility parameter L_x and integrating over the contact patch $\mathscr{C}$ (assumed, e.g., elliptical in shape) yields a relationship between the derivative of the longitudinal force and the longitudinal creepage[6]:

$$\dot{F}_x(t) = \frac{1}{L_x} \iint_{\mathscr{C}} \frac{\partial u_x(\boldsymbol{x}, t)}{\partial t} \, \mathrm{d}\boldsymbol{x} = -V(t) \frac{\pi ab}{L_x} \xi_x(t). \tag{43}$$

From Eq. (43), the longitudinal creepage may be expressed as an explicit function of the derivative $\dot{F}_x(t)$ as follows:

$$\xi_x = \frac{1}{V} \check{\xi}_x \left(\dot{F}_x \right) = -\frac{1}{V} \frac{L_x}{\pi ab} \dot{F}_x. \tag{44}$$

It is worth remarking that, according to Eqs. (43) and (44), the wheel-rail mechanical system behaves as a linear spring at low rolling speed. Indeed, integrating Eqs. (43) and (44) over time provides a linear relationship between the longitudinal force and the rigid displacement $V(t)\xi_x(t)$.

On the other hand, the second regime considers large values of $V(t)$. In this case, the partial derivative with respect to the longitudinal coordinate will be preponderant, giving

$$\frac{1}{V(t)} \frac{\partial u_x(\boldsymbol{x}, t)}{\partial t} - \frac{\partial u_x(\boldsymbol{x}, t)}{\partial x} \approx -\frac{\partial u_x(\boldsymbol{x}, t)}{\partial x} = -\xi_x(t), \qquad (\boldsymbol{x}, t) \in \mathscr{C} \times \mathbb{R}_{>0}. \tag{45}$$

Accordingly, by imposing the BC and integrating over $\mathscr{C}$ (assuming again no-slip conditions and an elliptical contact patch for simplicity), the classic steady-state relationship between the longitudinal force and the creepage may be derived to be of the form

$$F_x(t) = -\frac{8a^2 b}{3L_x} = -GabC_{11}\xi_x(t), \tag{46}$$

where a and b denote the semiaxes of the contact patch, and $C_{11} \triangleq 8a/(3L_x G)$ is the longitudinal *creep coefficient* (see Sect. 5.3.2). The algebraic relationship in Eq. (46) may be inverted yielding

$$\xi_x = \hat{\xi}_x(F_x) = -\frac{3L_x}{8a^2 b} F_x = -\frac{F_x}{GabC_{11}}. \tag{47}$$

---

[6]In the general case, assuming the deformation $\boldsymbol{u_\tau}(\boldsymbol{x}, t)$ to be a continuous function, it holds $\frac{\mathrm{d}}{\mathrm{d}t} \iint_{\mathscr{C}} \boldsymbol{u_\tau}(\boldsymbol{x}, t) \, \mathrm{d}\boldsymbol{x} = \iint_{\mathscr{C}} \frac{\partial \boldsymbol{u_\tau}(\boldsymbol{x}, t)}{\partial t} \, \mathrm{d}\boldsymbol{x}$, due to the boundary prescription and the assumption that the vertical pressure distribution vanishes at least on the trailing edge. The same result may be easily extended to a time-varying contact patch.

Equations (46) and (47) model the behaviour of the wheel-rail system as that of a linear damper at high rolling speeds. Combining Eqs. (44) and (47) allows expressing the longitudinal creepage as a weighted function of F_x and its time derivative $\dot{F}_x$, i.e.,

$$\xi_x = \frac{1}{V}\check{\xi}_x\left(\dot{F}_x\right) + \hat{\xi}_x(F_x) = -\frac{1}{V}\frac{L_x}{\pi ab}\dot{F}_x - \frac{F_x}{GabC_{11}}. \tag{48}$$

Equation (48) is a linear ODE for the time-varying longitudinal force, where the possibly time-varying input is the longitudinal creepage. In state space form [71], it may be more conveniently restated as

$$\dot{F}_x(t) = -V(t)\frac{\pi}{GC_{11}L_x}F_x(t) - V(t)\frac{\pi ab}{L_x}\xi_x(t) = -V(t)\frac{F_x(t)}{\lambda_{x\xi_x}} - V(t)\frac{GabC_{11}}{\lambda_{x\xi_x}}\xi_x(t), \tag{49}$$

where the *longitudinal relaxation length* has been defined as $\lambda_{x\xi_x} \triangleq GC_{11}L_x/\pi = 8a/(3\pi)$. It may be understood that the solution to the above equation derived under the assumption of no-slip conditions is stable, and converges asymptotically to unique dynamical equilibrium (obtained by setting $\dot{F}_x(t) = 0$ in Eq. (49)) that coincides with the steady-state value given by Eq. (46). From a physical viewpoint, the ODE (49) mimics the two different behaviours of the wheel-rail system, described using a linear spring and damper, respectively, occurring at low and high rolling speeds.

It is perhaps worth pointing out that the notion of relaxation length appears to be somewhat extraneous to the field of railway vehicle dynamics, whereas it is a well-established concept in road vehicle dynamics. In this paper, its introduction is propaedeutic to highlight some salient aspects connected with the so-called relaxation phenomena. In this context, it is instructive to consider the transient evolution of the longitudinal force for a wheel-rail system subjected, as already anticipated, to a constant longitudinal creepage input. More conveniently, and in analogy to what done for the original distributed model, when $V(t) > 0$, Eq. (49) may be converted into a time-invariant linear ODE by replacing the time variable t with the travelled distance q:

$$\frac{\mathrm{d}F_x(q)}{\mathrm{d}q} = -\frac{F_x(q)}{\lambda_{x\xi_x}} - \frac{GabC_{11}}{\lambda_{x\xi_x}}\xi_x(q). \tag{50}$$

The general solution to the above ODE (50) with IC $F_x(q_0) = F_{x0}$ reads

$$F_x(q) = F_{x0}\mathrm{e}^{-(q-q_0)/\lambda_{x\xi_x}} - \int_{q_0}^{q}\mathrm{e}^{-(q-q')/\lambda_{x\xi_x}}\frac{GabC_{11}}{\lambda_{x\xi_x}}\xi_x\left(q'\right)\mathrm{d}q', \tag{51}$$

which, in the case of constant longitudinal creepage, simplifies to

$$F_x(q) = F_{x0}\mathrm{e}^{-(q-q_0)/\lambda_{x\xi_x}} - GabC_{11}\xi_x\left(1 - \mathrm{e}^{-(q-q_0)/\lambda_{x\xi_x}}\right). \tag{52}$$

The implications of Eq. (52) are rather obvious: as predicted, for a constant creepage input, the longitudinal force converges asymptotically, and in fact exponentially, to the steady-state solution. More specifically, assuming $q_0 = 0$ for convenience, it may be deduced that the longitudinal force reaches the 96% of its stationary value after travelling a distance equal to $q = 3\lambda_{x\xi_x} = 8a/\pi \approx 2.5a$. This is in accordance to what observed experimentally, and already found in Sects. 3 and 4 concerning the distributed transient models. In view of this latter consideration, the example adduced above motivates a generalisation of the proposed approach, which is detailed in the next Sect. 5.2. Before moving to the derivation of the general theory, it is perhaps worth emphasising that the approximations in Eqs. (42) and (45) would ideally be exact at zero and infinite rolling speed, respectively. For any finite value of the latter, however low or high, the rolling contact dynamics would instead exhibit an intermediate behaviour between the two limit regimes. Actually, these should be interpreted as asymptotic behaviours that result from the mathematical structure of the governing PDEs (3).

5.2 General theory

So far, the analysis has been restricted to the simplified case of pure longitudinal creepage, which, in no-slip conditions, yields a linear relationship for the force in steady-state. However, the basic model may be easily modified to account for nonlinear effects occurring at high creepage values. Moreover, for the more general situation of combined longitudinal, lateral and spin creepages, the same idea may be extended by considering a first set of relationships describing $(\boldsymbol{\xi}, \phi)$ in terms of $(\boldsymbol{F_\tau}, M_z)$ as follows:

$$\boldsymbol{\xi} = \frac{1}{V}\check{\boldsymbol{\xi}}\left(\dot{\boldsymbol{F}}_{\boldsymbol{\tau}}, \dot{M}_z\right), \tag{53a}$$

$$\phi = \frac{1}{V}\breve{\phi}\left(\dot{\boldsymbol{F}}_{\boldsymbol{\tau}}, \dot{M}_z\right), \tag{53b}$$

where the functions $\breve{\boldsymbol{\xi}}(\cdot,\cdot) = [\breve{\xi}_x(\cdot,\cdot)\ \breve{\xi}_y(\cdot,\cdot)]^{\mathrm{T}}$ and $\breve{\phi}(\cdot,\cdot)$ are called *slip functions*, being reminiscent of the fact that, in integral form, they provide a set of equations relating the forces and moments with rigid displacements, that are basically the integral of the rigid slips. The derivation of the slip functions starting from the simplified theory is quite lengthy, and detailed for completeness in Appendix B.

On the other hand, in steady-state conditions, the explicit relationships between the tangential forces and the spin moment and the creepage variables are often known in the form

$$\boldsymbol{F}_{\boldsymbol{\tau}} = \hat{\boldsymbol{F}}_{\boldsymbol{\tau}}(\boldsymbol{\xi}, \phi), \tag{54a}$$

$$M_z = \hat{M}_z(\boldsymbol{\xi}, \phi), \tag{54b}$$

where $\hat{\boldsymbol{F}}_{\boldsymbol{\tau}}(\boldsymbol{\xi}, \phi)$, $\hat{M}_z(\boldsymbol{\xi}, \phi)$ are obtained by integration over $\mathscr{C}$ as in Eq. (10), or postulated according to some empirical model, like that indicated by Shen, Elkins and Hedrick (see Sect. 5.3.3). Inverting Eqs. (54) yields a local representation of the creepages $(\boldsymbol{\xi}, \phi)$ in the form of slip functions $(\hat{\boldsymbol{\xi}}, \hat{\phi})$, i.e.,

$$\boldsymbol{\xi} = \hat{\boldsymbol{\xi}}(\boldsymbol{F}_{\boldsymbol{\tau}}, M_z), \tag{55a}$$

$$\phi = \hat{\phi}(\boldsymbol{F}_{\boldsymbol{\tau}}, M_z), \tag{55b}$$

in which $\hat{\boldsymbol{\xi}}(\cdot,\cdot) = [\hat{\xi}_x(\cdot,\cdot)\ \hat{\xi}_y(\cdot,\cdot)]^{\mathrm{T}}$ and $\hat{\phi}(\cdot,\cdot)$ are referred to as steady-state *creepage functions* in this paper. It is worth remarking that Eqs. (53) and (55) are approximate in turn for low and high values of V. Interpolating between Eqs. (53) and (55) yields the two-regime transient models:

$$\boldsymbol{\xi} = \frac{1}{V}\breve{\boldsymbol{\xi}}\left(\dot{\boldsymbol{F}}_{\boldsymbol{\tau}}, \dot{M}_z\right) + \hat{\boldsymbol{\xi}}(\boldsymbol{F}_{\boldsymbol{\tau}}, M_z), \tag{56a}$$

$$\phi = \frac{1}{V}\breve{\phi}\left(\dot{\boldsymbol{F}}_{\boldsymbol{\tau}}, \dot{M}_z\right) + \hat{\phi}(\boldsymbol{F}_{\boldsymbol{\tau}}, M_z), \tag{56b}$$

Equations (56) allow expressing the creepages $(\boldsymbol{\xi}, \phi)$ as a weighted combination of two different vector-valued functions: the first captures the transient behaviour at low rolling speed, the second one, instead, gives an approximation at high rolling speeds. They also provide a set of ODEs for the creep forces. If the slip functions have an isolated equilibrium at the origin, it is clear that the equilibria of the ODEs (56) coincide with the steady-state relationships for the creepage-force laws.

In Appendix B, it is shown that the slip functions are, in fact, linear, and therefore the system in Eqs. (56) may be restated in state-space form according to

$$\begin{bmatrix} \dot{\boldsymbol{F}}_{\boldsymbol{\tau}}(t) \\ \dot{M}_z(t) \end{bmatrix} = -V(t) \begin{bmatrix} \mathbf{L}'_{\boldsymbol{F}} & \mathbf{L}'_M \\ \mathbf{L}'_{\phi\boldsymbol{F}} & L'_{\phi M} \end{bmatrix}^{-1} \begin{bmatrix} \boldsymbol{\xi} - \hat{\boldsymbol{\xi}}\left(\boldsymbol{F}_{\boldsymbol{\tau}}(t), M_z(t)\right) \\ \phi - \hat{\phi}\left(\boldsymbol{F}_{\boldsymbol{\tau}}(t), M_z(t)\right) \end{bmatrix}, \tag{57}$$

where the matrix on the right-hand side is nonsingular, and $\mathbf{L}'_{\boldsymbol{F}}$, $\mathbf{L}'_M$, $\mathbf{L}'_{\phi\boldsymbol{F}}$ and $L'_{\phi M}$ represent generalised flexibilities. Moreover, Eq. (57) may be reinterpreted in terms of relaxation lengths as follows:

$$\begin{bmatrix} \boldsymbol{\Lambda}_{\boldsymbol{\xi}} & \boldsymbol{\Lambda}_{\phi} \\ \boldsymbol{\Lambda}_{M\boldsymbol{\xi}} & \lambda_{M\phi} \end{bmatrix} \begin{bmatrix} \dot{\boldsymbol{F}}_{\boldsymbol{\tau}}(t) \\ \dot{M}_z(t) \end{bmatrix} = -V(t)Gab\mathbf{C}_{\boldsymbol{\tau}} \begin{bmatrix} \boldsymbol{\xi} - \hat{\boldsymbol{\xi}}\left(\boldsymbol{F}_{\boldsymbol{\tau}}(t), M_z(t)\right) \\ \phi - \hat{\phi}\left(\boldsymbol{F}_{\boldsymbol{\tau}}(t), M_z(t)\right) \end{bmatrix}, \tag{58}$$

where a and b are two characteristic geometrical parameters, $\mathbf{C}_{\boldsymbol{\tau}}$ is a matrix of creep coefficients[7], and

$$\begin{bmatrix} \boldsymbol{\Lambda}_{\boldsymbol{\xi}} & \boldsymbol{\Lambda}_{\phi} \\ \boldsymbol{\Lambda}_{M\boldsymbol{\xi}} & \lambda_{M\phi} \end{bmatrix} = \begin{bmatrix} \lambda_{x\xi_x} & \lambda_{x\xi_y} & \lambda_{x\phi} \\ \lambda_{y\xi_x} & \lambda_{y\xi_y} & \lambda_{y\phi} \\ \lambda_{M\xi_x} & \lambda_{M\xi_y} & \lambda_{M\phi} \end{bmatrix} \triangleq Gab\mathbf{C}_{\boldsymbol{\tau}} \begin{bmatrix} \mathbf{L}'_{\boldsymbol{F}} & \mathbf{L}'_M \\ \mathbf{L}'_{\phi\boldsymbol{F}} & L'_{\phi M} \end{bmatrix}. \tag{59}$$

Whilst a major advantage of the two-regime approach undoubtedly resides in its pure analytical nature, its major limitation consists in the fact an explicit representations as in Eq. (55) might often be obtained only locally. This aspect will be perhaps clarified better in the subsequent Sect. 5.3, where the slip and creepage functions will be derived. Before proceeding to the introduction of the approximated transient models, it is worth emphasising that the parameters collected in the matrices appearing in Eqs. (57), (58),

---

[7]For example, for an elliptical contact patch, and according to Kalker's exact and simplified theories, it would read as in Sect. 5.3.2 even in the nonlinear case.

and (59) may be generally time-varying, implying that the formulae derived above hold very general. In fact, since the derivation conducted in Appendix B does not rely on any specific assumption (apart from being grounded on the simplified theory), the two-regime theory may be realised to be valid independently of the contact patch shape, which may also be allowed to be time-varying[8].

5.3 Analytical two-regime transient models

Three different creep-forces relationships are reviewed in this paper: Carter's model [40], Kalker's linear model [4], and the enhanced formulation developed by Shen, Elkins and Hedrick [42]. The analytical relationships derived by considering Kalker's simplified theory are not introduced directly, since these might be interpreted as particular cases of Kalker's linear model and Shen, Elkins and Hedrick's model. Other formulations, like the elegantly simple model proposed by Polach [67], are not explicitly considered in this paper owing to the difficulties connected with the analytical inversion of the corresponding creepage functions. On the other hand, possible extensions to include falling friction effects, like those documented in [68, 69], may instead be immediate.

All the transient models discussed in the following have not been presented before.

5.3.1 Transient Carter's model

Carter was the first to derive a closed form solution for the stress acting inside the contact patch, under the assumptions of steady rolling and pure longitudinal creepage [40]. His solution is also restricted to the case of line contact. According to Carter, a closed-form expression for the longitudinal traction may be deduced as

$$F_x = \hat{F}_x(\xi_x) = -\mu F_z \left[1 - \left(1 - \frac{|\xi_x|}{\xi^{\mathrm{cr}}} \right)^2 \right] \operatorname{sgn} \xi_x, \qquad\qquad |\xi_x| \in [0, \xi^{\mathrm{cr}}), \qquad (60)$$

where ξ^{cr} denotes the critical value for which the creep-force law saturates, that is $\xi^{\mathrm{cr}} \triangleq \mu a/R$.

The inverse relationship of Eq. (60) reads obviously

$$\xi_x = \hat{\xi}_x(F_x) = -\xi^{\mathrm{cr}} \left(1 - \sqrt{1 - \frac{|F_x|}{\mu F_z}} \right) \operatorname{sgn} F_x, \qquad\qquad |F_x| \in [0, \mu F_z). \qquad (61)$$

Combining the slip function with the expression in Eq. (61), the following nonlinear ODE may be established:

$$\dot{F}_x(t) = -V(t) C'_{\xi_x} \left[\xi_x(t) + \xi^{\mathrm{cr}} \left(1 - \sqrt{1 - \frac{|F_x(t)|}{\mu F_z}} \right) \operatorname{sgn}\big(F_x(t)\big) \right], \qquad (62)$$

with $C'_{\xi_x} \triangleq A_{\mathscr{C}}/L_x$, being $A_{\mathscr{C}}$ the area of the contact patch as defined in Eq. (104a) (Appendix B).

For the model under consideration, asymptotic and input-to-state stability [70] may be easily verified by considering the candidate Lyapunov function $V(F_x(t)) = \frac{1}{2} F_x^2(t)$. Calculating the time derivative $\dot{V}(F_x(t))$ it may be deduced that any value of $F_x(t)$ satisfying

$$\xi^{\mathrm{cr}} \left(1 - \sqrt{1 - \frac{|F_x(t)|}{\mu F_z}} \right) \geq \frac{|\xi_x(t)|}{\psi} \qquad (63)$$

for some values of $\psi \in (0, 1)$ arbitrarily close to the unity ensures $\dot{V}(F_x(t))$ to be negative definite. Reversing the inequality, it may be inferred that if

$$\sup_{t \geq t_0} |\xi_x(t)| < \psi \xi^{\mathrm{cr}}, \qquad (64)$$

then $|F_x(t)| < \mu F_z$ for all $t \geq t_0$.

---

[8]This important property is a direct consequence of the fact that, according to the simplified theory discussed in Sect. 4, the deformation is a continuous function of the longitudinal coordinate, and the tangential stresses must necessarily vanish at the trailing edge.

5.3.2 Transient Kalker's linear model

In combined creepage conditions, that is $(\boldsymbol{\xi}, \phi) \neq (\mathbf{0}, 0)$, it is not possible to recover a closed-form expression for the tractions and the spin moment acting at the contact patch. For many cases of practical interest, approximated description may be derived by linearisation in a neighbourhood of the origin, as suggested by Kalker [4]. This leads to the following relationship between the tractions $(\boldsymbol{F}_{\boldsymbol{\tau}}, M_z)$ and the creepage variables $(\boldsymbol{\xi}, \phi)$:

$$\begin{bmatrix} \boldsymbol{F}_{\boldsymbol{\tau}} \\ M_z \end{bmatrix} = \begin{bmatrix} \hat{\boldsymbol{F}}_{\boldsymbol{\tau}}(\boldsymbol{\xi}, \phi) \\ \hat{M}_z(\boldsymbol{\xi}, \phi) \end{bmatrix} = -Gab\mathbf{C}_{\boldsymbol{\tau}} \begin{bmatrix} \boldsymbol{\xi} \\ \phi \end{bmatrix}, \tag{65}$$

where the matrix $\mathbf{C}_{\boldsymbol{\tau}}$ reads specifically

$$\mathbf{C}_{\boldsymbol{\tau}} = \begin{bmatrix} C_{11} & 0 & 0 \\ 0 & C_{22} & \sqrt{ab}C_{23} \\ 0 & -\sqrt{ab}C_{23} & abC_{33} \end{bmatrix}. \tag{66}$$

The entries of the matrix $\mathbf{C}_{\boldsymbol{\tau}}$ are usually called *creep coefficients* or *Kalker coefficients*, and are tabulated for different values of the semiaxis relation and Poisson ratio.

The inverse relationship of Eq. (65) may be derived simply as

$$\begin{bmatrix} \boldsymbol{\xi} \\ \phi \end{bmatrix} = \begin{bmatrix} \hat{\boldsymbol{\xi}}(\boldsymbol{F}_{\boldsymbol{\tau}}, M_z) \\ \hat{\phi}(\boldsymbol{F}_{\boldsymbol{\tau}}, M_z) \end{bmatrix} = -\frac{1}{Gab}\mathbf{C}_{\boldsymbol{\tau}}^{-1} \begin{bmatrix} \boldsymbol{F}_{\boldsymbol{\tau}} \\ M_z \end{bmatrix}, \tag{67}$$

with

$$\mathbf{C}_{\boldsymbol{\tau}}^{-1} = \begin{bmatrix} \dfrac{1}{C_{11}} & 0 & 0 \\ 0 & \dfrac{C_{33}}{C_{23}^2 + C_{22}C_{33}} & -\dfrac{C_{23}}{\sqrt{ab}C_{23}^2 + \sqrt{ab}C_{22}C_{33}} \\ 0 & \dfrac{C_{23}}{\sqrt{ab}C_{23}^2 + \sqrt{ab}C_{22}C_{33}} & \dfrac{C_{22}}{abC_{23}^2 + abC_{22}C_{33}} \end{bmatrix}. \tag{68}$$

In this case, the two-regime transient model may be inferred to be of the form

$$\begin{bmatrix} \dot{\boldsymbol{F}}_{\boldsymbol{\tau}}(t) \\ \dot{M}_z(t) \end{bmatrix} = -V(t) \begin{bmatrix} \mathbf{L}'_{\boldsymbol{F}} & \mathbf{L}'_M \\ \mathbf{L}'_{\phi\boldsymbol{F}} & L'_{\phi M} \end{bmatrix}^{-1} \left(\begin{bmatrix} \boldsymbol{\xi}(t) \\ \phi(t) \end{bmatrix} + \frac{\mathbf{C}_{\boldsymbol{\tau}}^{-1}}{Gab} \begin{bmatrix} \boldsymbol{F}_{\boldsymbol{\tau}}(t) \\ M_z(t) \end{bmatrix} \right). \tag{69}$$

In the present case, the resulting formulation consists of a linear system of ODEs, and the stability properties of the model may be easily inferred by checking the eigenvalues of the corresponding homogeneous equations [71].

For an elliptical contact patch, the equivalent linear relationships according to the simplified theory in no slip-conditions, obtained by integration of the steady-state version of Eqs. (21) all over $\mathscr{C}$, may be derived directly from the model (65) by specifying the creep coefficients appearing in Eq. (66) as follows:

$$C_{11} \equiv C_{22} = \frac{8a}{3LG}, \qquad \text{and} \qquad C_{23} = \frac{\pi a^2}{4LG\sqrt{ab}}. \tag{70}$$

Similar equivalences also hold for different geometries like the *simple double-elliptical contact* (SDEC) patch proposed by Piotrowski, Liu and Bruni [72] (see the discussions in, e.g., [73, 74]).

5.3.3 Transient Shen, Elkins and Hedrick's model

Johnson attempted to extend the exact solution derived by Carter to the more general case of combined creepage conditions [75, 76]. He proposed an approximated solution for a circular contact patch. Later on, the result was generalised to an elliptical geometry by Vermeulen and Johnson [77].

In the same spirit, Shen, Hedrick and Elkins suggested to adopt the creep coefficients appearing in the matrix $\mathbf{C}_{\boldsymbol{\tau}}$ to better replicate the initial slope of the creepage-force relationship [42]. They also included the contribution of the spin, although disregarding the influence of the spin moment. The following analysis is limited to the simpler situation of combined translational creepages, and neglects the spin.
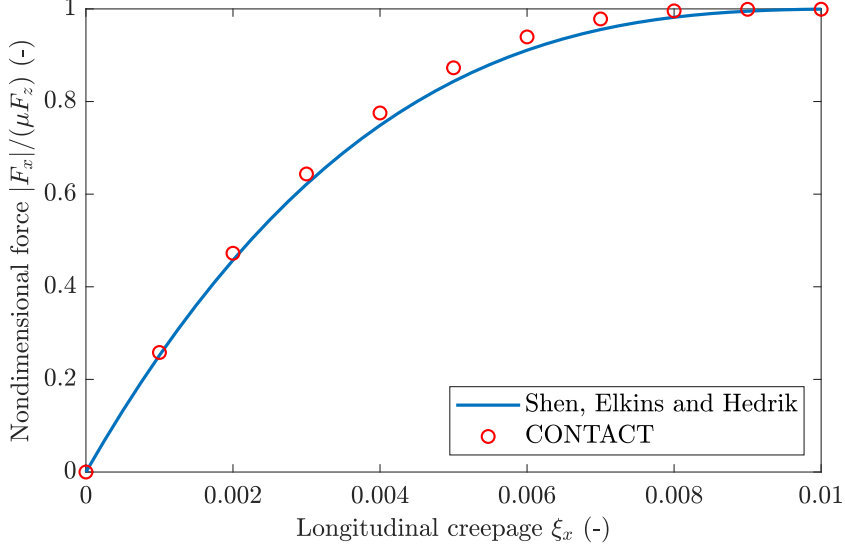
Figure 2: Comparison between the nondimensional longitudinal force-creepage characteristic $|F_x|/(\mu F_z)$ predicted by Shen, Elkins and Hedrik's formula and CONTACT. Parameters: $a = b = 0.0035$ m, $F_z = 15$ kN, $\mu = 0.4$.

Thus, introducing the modified creepages $\tilde{\boldsymbol{\xi}} \triangleq [C_{11}\xi_x \; C_{22}\xi_y]^\mathrm{T}$ and $\tilde{\xi} \triangleq \left\|\tilde{\boldsymbol{\xi}}\right\|$, the following formula is considered

$$\boldsymbol{F_\tau} = \hat{\boldsymbol{F}}_\tau\left(\tilde{\boldsymbol{\xi}}\right) = \hat{F}_\tau\left(\tilde{\xi}\right)\frac{\tilde{\boldsymbol{\xi}}}{\tilde{\xi}} = -\mu F_z\left[1 - \left(1 - \frac{\tilde{\xi}}{\tilde{\xi}^\mathrm{cr}}\right)^3\right]\frac{\tilde{\boldsymbol{\xi}}}{\tilde{\xi}}, \qquad \tilde{\xi} \in [0, \tilde{\xi}^\mathrm{cr}), \tag{71}$$

where this time the modified critical creepage value is defined as $\tilde{\xi}^\mathrm{cr} \triangleq 3\mu F_z/(abG)$. A comparison between the force-creepage characteristic predicted by Shen, Elkins and Hedrik's model and Kalker's exact theory is illustrated in Fig. 2 for completeness.

According to Eq. (71), the inverse relationship may be found in the form

$$\boldsymbol{\xi} = \hat{\boldsymbol{\xi}}(\boldsymbol{F_\tau}) = -\begin{bmatrix} \dfrac{1}{C_{11}} & 0 \\ 0 & \dfrac{1}{C_{22}} \end{bmatrix} \tilde{\xi}^\mathrm{cr}\left(1 - \sqrt[3]{1 - \frac{F_\tau}{\mu F_z}}\right)\frac{\boldsymbol{F_\tau}}{F_\tau}, \qquad F_\tau \in [0, \mu F_z), \tag{72}$$

being C_{11} and C_{22} the creep coefficients appearing in the matrix $\mathbf{C}_\tau$ already introduced in Sect. 5.3.2.

The two-regime model may thus be deduced to be of the form

$$\dot{\boldsymbol{F}}_\tau(t) = -V(t)\left[\mathbf{C}'_{\boldsymbol{\xi}}\boldsymbol{\xi}(t) + \frac{3A_\mathscr{C}G}{8a}\tilde{\xi}^\mathrm{cr}\left(1 - \sqrt[3]{1 - \frac{F_\tau(t)}{\mu F_z}}\right)\frac{\boldsymbol{F}_\tau(t)}{F_\tau(t)}\right], \tag{73}$$

where

$$\mathbf{C}'_{\boldsymbol{\xi}} = \begin{bmatrix} C'_{\xi_x} & 0 \\ 0 & C'_{\xi_y} \end{bmatrix} \triangleq \mathbf{L}'^{-1}_{\boldsymbol{F}} = A_\mathscr{C}\begin{bmatrix} \dfrac{1}{L_x} & 0 \\ 0 & \dfrac{1}{L_y} \end{bmatrix}, \tag{74}$$

and it has been assumed that the the entries of $\mathbf{L}_\tau$ are chosen so as to match the exact solution in the linear region, that is $L_x = 8a/(3C_{11}G)$ and $L_y = 8a/(3C_{22}G)$. Following a similar reasoning to that in Sect. 5.3.1, it may be shown that input-to-state stability (i.e., also $F_\tau(t) < \mu F_z$) is guaranteed when

$$\sup_{t \geq t_0} \xi(t) < \frac{\psi\tilde{\xi}^\mathrm{cr}}{\max\{C_{11}, C_{22}\}}, \tag{75}$$

16

for any $\psi \in (0,1)$ arbitrarily close to the unity. From the values tabulated by Kalker, $C_{11} = 4.25$ is usually greater than $C_{22} = 3.67$, and therefore it may be concluded that input-to-state stability properties are mainly limited by the longitudinal creep coefficient. In this context, it is important to clarify that the bound in Eq. (75) has been imposed following the classic definition of input-to-state stability, whereas, for the model under consideration, it is also possible to account for the directionality of the input, as discussed more extensively in [39].

According to Kalker's simplified theory, assuming $L_x = L_y = L$, a similar relationship for line contact may be derived as in Eq. (73) by formally specifying $C_{11} = C_{22} = 1$. In this case, Eq. (75) implies that input-to-state stability properties are guaranteed for any value of the total creepage smaller than the critical one, with $\tilde{\xi}^{\mathrm{cr}} \triangleq 3\mu F_z L/(4a^2)$.

6 Comparison between different theories

The present section is devoted to the comparison of the three theories previously discussed. In particular, the linear theories are equivalent at least in steady-state, provided that the model parameters are correctly specified. The comparison is therefore performed concerning the simplified theory developed by Kalker with the corresponding two-regime formulation introduced in Sect. 5.3.2.

On the other hand, the exact description of the rolling contact mechanics based on the theory of elasticity is compared to the two-regime models according to the variants presented in Sects. 5.3.1 and 5.3.3, respectively, for the cases of line contact and elliptical patch with combined creepages.

In the following analysis, the travelled distance q is adopted as independent variable in place of the time t, so as to render the problem independent of the rolling velocity.

6.1 Linear theories

Two separate cases are covered: the first one considers the effect of combined creepages and spin, whereas the second investigates the influence of a time-varying normal load and longitudinal creepage.

6.1.1 Combined creepages and spin

Assuming a constant contact patch and no-slip conditions, the transient problem may be easily solved concerning Kalker's simplified theory. In particular, the time-varying deformations $\boldsymbol{u_\tau}(\boldsymbol{x}, q)$ may be immediately deduced by combining Eqs. (25), (26) and (27). Recalling the linear constitutive relationship in Eq. (18) and integrating according to Eqs. (9) provides the trend of the tangential forces and moment predicted using the distributed representation.

The two-regime model, reformulated replacing the time variable t with the travelled distance q, reads

$$\frac{\mathrm{d}}{\mathrm{d}q}\begin{bmatrix} \boldsymbol{F_\tau}(q) \\ M_z(q) \end{bmatrix} = -\begin{bmatrix} \mathbf{L}'_{\boldsymbol{F}} & \mathbf{L}'_M \\ \mathbf{L}'_{\phi\boldsymbol{F}} & L'_{\phi M} \end{bmatrix}^{-1}\left(\begin{bmatrix} \boldsymbol{\xi}(q) \\ \phi(q) \end{bmatrix} + \frac{\mathbf{C}_{\boldsymbol{\tau}}^{-1}}{Gab}\begin{bmatrix} \boldsymbol{F_\tau}(q) \\ M_z(q) \end{bmatrix}\right), \tag{76}$$

and needs to be supplemented with ICs $\boldsymbol{F}_{\boldsymbol{\tau}0} = \boldsymbol{F_\tau}(0)$ and $M_{z0} = M_z(0)$ compatible with the initial distribution $\boldsymbol{u}_{\boldsymbol{\tau}0}(\boldsymbol{x})$. The solution to the linear system (76) may be computed in closed-form as

$$\begin{bmatrix} \boldsymbol{F_\tau}(q) \\ M_z(q) \end{bmatrix} = \boldsymbol{\Phi_\tau}(q,0)\begin{bmatrix} \boldsymbol{F}_{\boldsymbol{\tau}0} \\ M_{z0} \end{bmatrix} - \int_0^q \boldsymbol{\Phi_\tau}(q,q')\begin{bmatrix} \mathbf{L}'_{\boldsymbol{F}} & \mathbf{L}'_M \\ \mathbf{L}'_{\phi\boldsymbol{F}} & L'_{\phi M} \end{bmatrix}^{-1}\begin{bmatrix} \boldsymbol{\xi}(q') \\ \phi(q') \end{bmatrix}\mathrm{d}q', \qquad q \in \mathbb{R}_{\geq 0}, \tag{77}$$

where the transition matrix $\boldsymbol{\Phi_\tau}(q,\tilde{q})$ may be determined as

$$\boldsymbol{\Phi_\tau}(q,\tilde{q}) = \exp\left(-\begin{bmatrix} \mathbf{L}'_{\boldsymbol{F}} & \mathbf{L}'_M \\ \mathbf{L}'_{\phi\boldsymbol{F}} & L'_{\phi M} \end{bmatrix}^{-1}\frac{\mathbf{C}_{\boldsymbol{\tau}}^{-1}}{Gab}(q - \tilde{q})\right). \tag{78}$$

The entries of the transition matrix, which is indeed a matrix exponential, may be calculated in closed-form, but their expression is rather lengthy and not reported here for brevity. Instead, the comparison between the transient characteristics computed according to the two models is shown in Fig. 3, limitedly to the case of constant creepage inputs. In general, it may be observed that the two-regime theory (solid lines) predicts a slightly slower convergence to the steady-state values than the simplified theory. In any case, the agreement is encouragingly good, and the analysis may be easily extended to the more general situation of varying creepages, as testified by the subsequent investigation conducted in Sect. 6.1.2.
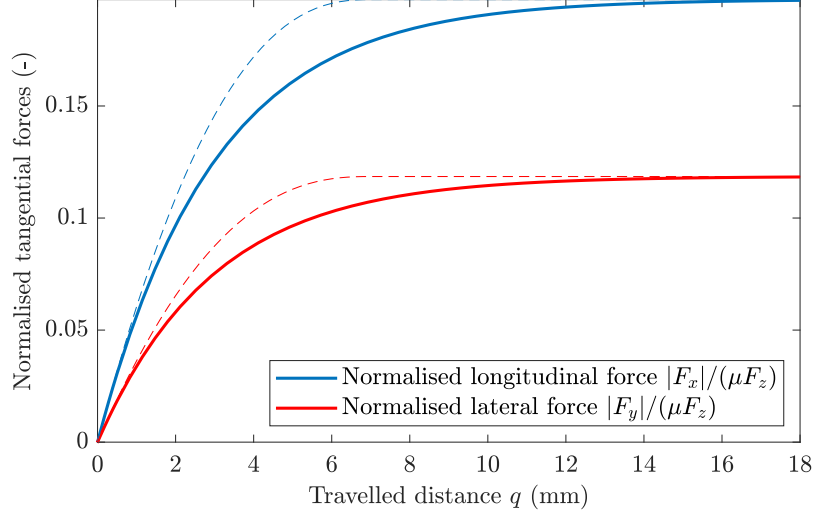
(a) Nondimensional tangential forces $|F_x|/(\mu F_z), |F_y|/(\mu F_z)$.
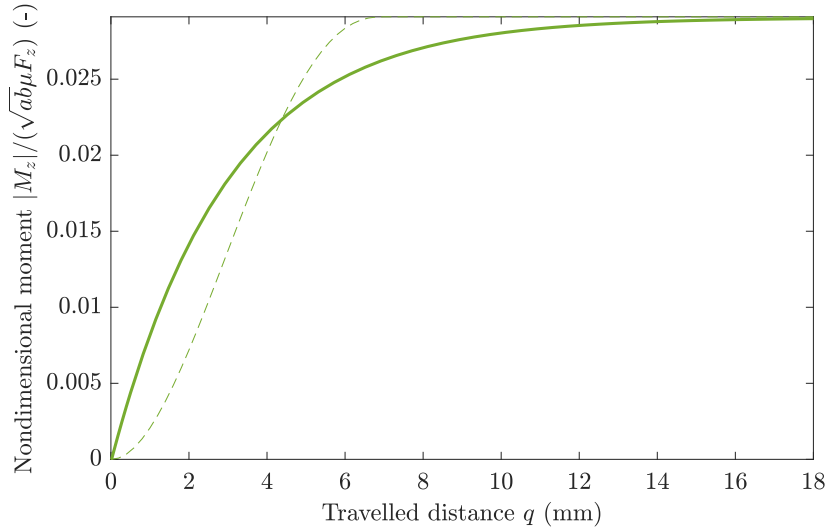
(b) Nondimensional spin moment $|M_z|/(\sqrt{ab}\mu F_z)$.

Figure 3: Transient evolution of the nondimensional tangential forces and moment $|F_x|/(\mu F_z), |F_y|/(\mu F_z)$, $|M_z|/(\sqrt{ab}\mu F_z)$ for a wheel subjected to constant creepage and spin inputs of $\xi_x = 0.0005$, $\xi_y = 0.0003$ and $\phi = 0.0001$ according to the two-regime theory (solid lines) and Kalker's simplified theory (dashed lines). Other parameters are specified as follows: $a = b = 0.0035$ m, $F_z = 15$ kN, $\mu = 0.4$.

6.1.2 Time-varying contact patch

In this paper, the more general situation of time-varying contact patch is considered due to its relevance concerning the investigation of short-pitch corrugation phenomena, connected with oscillating normal forces [22–24]. In particular, it is conjectured in [22] that harmonic excitations produced by time-varying creepages may constitute a potential source of dynamical instability. The present analysis attempts therefore at evaluating the contribution of harmonic creepages upon the mechanism of transient generation of wheel-rail contact forces. The example adduced below, limited for simplicity to the case of line contact under no-slip assumptions, is mainly illustrative, and inspired by the interesting analysis conducted by Barber [22], where it is shown that a periodic vertical load of the form $F_z(q) = F_{z0} + F_{zI}\sin(\omega_q q)$ typically induces similar fluctuations in the contact semilength and longitudinal creepage. Owing to the hypotheses outlined above, after a suitable transformation of variables, the distributed problem may be described using the PDE (39), supplemented opportunely with BC and IC given by Eqs. (40) and (41), and parameters reading specifically

$$a(q) = a_0 + a_I \sin(\omega_q q), \tag{79a}$$

$$\xi_x(q) = \xi_0 + \xi_I \sin(\omega_q q), \tag{79b}$$

where ω_q has the same dimension of a curvature, and represent a spatial frequency accounting for rail irregularities. Obviously, the identities $a(q) \equiv a(\tilde{q})$ and $\xi(q) \equiv \tilde{\xi}(\tilde{q})$ hold. Moreover, the two conditions $a_I < a_0$ and $\omega_q a_I < 1$ clearly ensure the BC (40) to be noncharacteristic. The transient deformation $\tilde{u}_x(\tilde{x}, \tilde{q})$ may be calculated numerically, and then the longitudinal force may be determined using the formula in Eq. (101a), according to the approach detailed in Appendix A.

On the other hand, for the problem under consideration, the two-regime linear model simplifies to

$$\frac{\mathrm{d}F_x(q)}{\mathrm{d}q} = -\frac{F_x(q)}{a(q)} - \frac{2a(q)}{L_x}\xi_x(q). \tag{80}$$

The above Eq. (80) may be deduced directly from Eq. (69), by neglecting the contribution of the lateral and spin creepages, and recalling that $C_{11} = C_{11}(q) = 2a(q)/(GL_x)$ under the assumption of line contact. By noticing that $\mathscr{C}_0 \triangleq \mathscr{C}(0) = \{x \in \mathbb{R} \mid -a_0 \le x \le a_0\}$, the analytical solution to the ODE (80) equipped with IC given by

$$\text{IC:} \qquad F_x(0) = F_{x0} = \int_{\mathscr{C}_0} \frac{u_{x0}(x)}{L_x}\,\mathrm{d}x \tag{81}$$

reads explicitly

$$F_x(q) = F_{x0}\exp\left(-\int_0^q \frac{1}{a(q')}\,\mathrm{d}q'\right) - \int_0^q \exp\left(-\int_{q'}^q \frac{1}{a(\tilde{q})}\,\mathrm{d}\tilde{q}\right)\frac{2a(q')}{L_x}\xi_x(q')\,\mathrm{d}q', \qquad q \in \mathbb{R}_{\ge 0}. \tag{82}$$

The comparison between the transient longitudinal forces predicted according to the two theories is illustrated in Fig. 4 for three different combinations of creepages $\xi_x(q)$ and spatial frequencies ω_q. Again, it may be generally observed a very good agreement between the distributed description, formulated in terms of a PDE, and two-regime model, which confirms the validity of the hypotheses underlying the derivation of the latter.

In reality, due to the relatively fast harmonic excitation, the effect of a time-varying creepage appears to be negligible upon the transient phenomenon, as illustrated in greater detail in Fig. 5, where the evolution of the tangential forces is reported concerning the first eight centimeters of travelled distance q. Indeed, after an initial discrepancy between the unsteady trends predicted according to the simplified and two-regime theories and the corresponding steady-state values (dash-dotted lines), the match is almost perfect immediately after convergence. This result seems to suggests that the steady-state approximation is reasonable even when dealing with transient phenomena induced by corrugation, at least in the examined range of creepage values and excitation frequencies.

6.2 Nonlinear theories

The nonlinear theories presented in this paper cover the exact solution derived by Kalker for the case of line contact and the approximated model proposed by Shen, Elkins and Hedrick. Since the usefulness of the transient analysis under the assumption of line contact is mostly limited to pedagogical applications, only the latter is compared to the two-regime formulation.
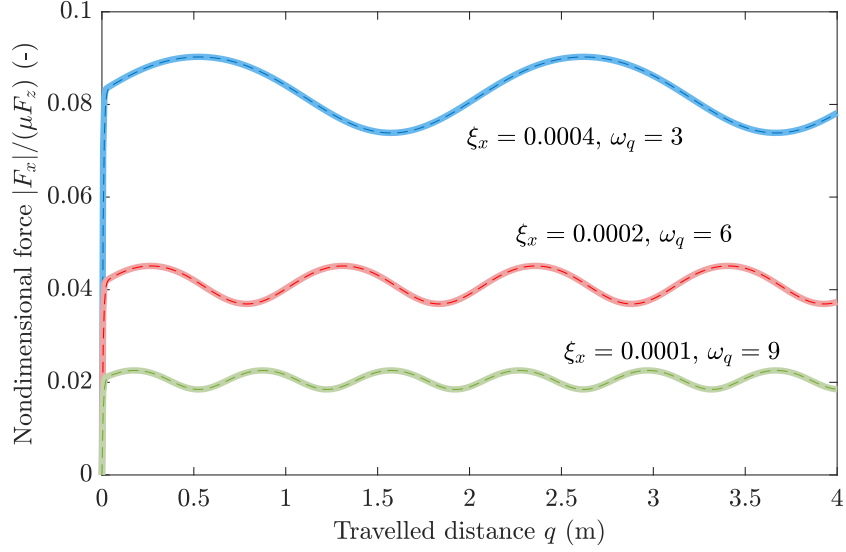
Figure 4: Transient evolution of the nondimensional longitudinal force $|F_x|/(\mu F_z)$ depending on different combinations of creepages ξ_x and spatial frequencies ω_q according to the two-regime theory (solid lines) and Kalker's simplified theory (dashed lines). The varying component ξ_I of the creepage is always set to $\xi_I = 0.1 \cdot \xi_0$. Other parameters are specified as follows: $a_0 = 0.0035$ m, $a_I = 0.0005$ m, $L_x = 7.86 \cdot 10^{-12}$ m^2 N.

Figure 5: Transient evolution of the nondimensional longitudinal force $|F_x|/(\mu F_z)$ depending on different combinations of creepages ξ_x and spatial frequencies ω_q according to Kalker's simplified theory (solid lines), the two-regime theory (dashed lines), and the steady-state approximation (dash-dotted lines). The varying component ξ_I of the creepage is always set to $\xi_I = 0.1 \cdot \xi_0$. Other parameters are specified as follows: $a_0 = 0.0035$ m, $a_I = 0.0005$ m, $L_x = 7.86 \cdot 10^{-12}$ m^2 N.
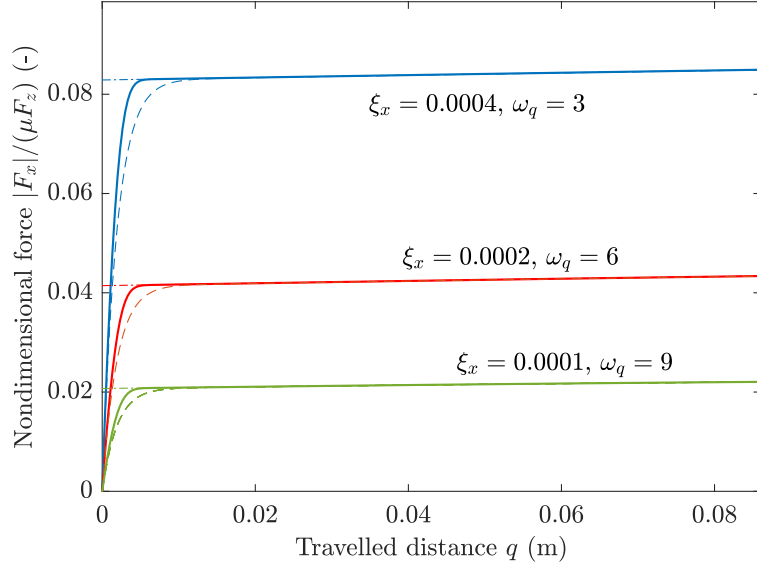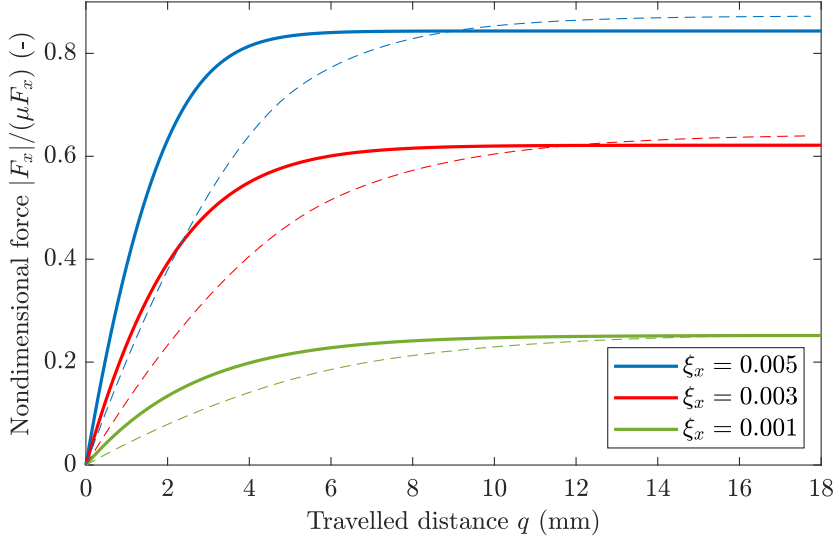
Figure 6: Transient evolution of the nondimensional longitudinal force $|F_x|/(\mu F_z)$ for a wheel subjected to constant longitudinal creepage inputs of $\xi_x = 0.005$, 0.003 and 0.001, respectively, according to the two-regime theory (solid lines) and CONTACT (dashed lines). Other parameters are specified as follows: $a = b = 0.0035$ m, $F_z = 15$ kN, $\mu = 0.4$.

6.2.1 Longitudinal creepage

When the creepages are relatively high, the two-regime model based on Shen, Elkins, and Hedrik's formula may be more conveniently adopted. For simplicity, the following example restricts to the case of a wheel subjected to constant longitudinal creepage inputs. Owing to the complex nonlinear nature of Eq. (73), a closed-form solution cannot be obtained concerning the evolution equation for the tangential forces. However, input-to-state stability holds as far as the criterion in Eq. (75) is fulfilled.

Figure 6 compares the transient force generated at the wheel-rail interface in response to a step input for three values of the creepage $\xi_x = 0.005$, 0.003 and 0.001, respectively, according to the two-regime model (solid line) and CONTACT (dashed line), which is based on Kalker's exact theory. Apart from a discrepancy in the velocity of the transients, another difference between the two theories relates to the fact that Shen, Elkins, and Hedrik's model does not match the theoretical force-creepage characteristic in steady-state conditions, especially concerning the nonlinear region. Qualitatively, the transient phenomena are however well-replicated by the latter formulation, which may be also modified to accommodate a slower convergence to the steady-state values by introducing a corrective factor multiplying the right-hand side of Eq. (73).

7 Conclusions

The present paper has explored transient phenomena occurring in wheel-rail rolling contact according to three different theories: the exact model based on the theory of elasticity, the simplified model that adopts a Winkler approximation, and the two-regime model recently introduced in [39]. The first two theories describe wheel-rail contact phenomena using a distributed representation, that is, a set of PDEs; the third approach consists instead in a pragmatic approximation that regards the forces and moments acting mutually between the wheel and rail interface as a (possibly nonlinear) dynamical system, described, i.e., in terms of simpler ODEs.

In particular, concerning a distributed representation of the wheel-rail interaction, the focus has principally been on Kalker's simplified theory, which, whilst still allowing for an analytical approach, simultaneously appears to be sufficiently adequate to explain the salient effects connected with variations in creepages and oscillating vertical forces. In fact, it is remarkable how even Johnson pointed out the unsurmountable difficulties connected with a rigorous investigation within the framework of the exact theory [8], which has so far limited the analysis to the rather restrictive case of line contact and longitudinal creepage. On the other hand, the majority of the nonlinear phenomena connected with

transient dynamics may be easily studied using the simplified theory, including the more involved cases of time-varying creepages and normal loads. In the context of railway studies, the results advocated in this paper are essentially novel, particularly concerning the analysis carried out in Sect. 4.3 with respect to a time-varying contact patch.

As already mentioned, the simplified theory, however simple, still relies on a distributed representation of the wheel-rail interaction. In the context of railway dynamics studies, this might easily become problematic, given the possibly large number of coupled equations needed to describe the motion of different vehicle subsystems [36]. An alternative is therefore to approximate the PDEs of the simplified theory by resorting to an order reduction approach. The two-regime model addresses this problem by interpolating between two different behaviours that the wheel-rail system exhibits at low and high rolling speed, respectively. By combining two set of equations, the resulting dynamics is pragmatically approximated using a lumped model, which is entirely analytical and describes the transient evolution of the tangential forces and moments depending on the creepage inputs. The ODEs for the two-regime model may be easily derived from already-existing creepage-force relationships available from the literature. More specifically, in this paper, three formulations have been considered departing from the linear model developed by Kalker [7], the famous Carter's solution [40], and the enhanced formula proposed by Shen, Elkins and Hedrick [42]. The two-regime models developed in the paper have been compared to the corresponding distributed theories, showing an encouragingly good agreement, although not perfect. The match may anyway be improved by introducing corrective factors on the right-hand sides of the two-regime equations without altering the original equilibria. However, such possibility has not been considered directly in this paper and is deferred to future studies.

The findings of the present investigation may be used to conduct stability analyses of entire vehicle systems and subsystems considering the transient dynamics of the wheel-rail contact, whereas a quasi-static approach is often preferred. In fact, unsteady phenomena may be expected to represent an additional source of instability, as suggested for example in [22–24] in the context of corrugation studies. Moreover, whilst the pragmatic ODE-based models introduced in this paper are exclusively based on the simplified theory of rolling contact, other approximations may be derived directly departing from the exact theory of elasticity. Some efforts in this direction have already been done by other scholars [16, 66], but further research is needed.

Compliance with Ethical Standards

The authors declare that they have no conflict of interest.

Nomenclature

Forces and Moments	Unit	Description
$\boldsymbol{F_\tau}$	N	Tangential force vector
$\boldsymbol{F_{\tau 0}}$	N	Initial conditions for the tangential force vector
F_x, F_y	N	Longitudinal and lateral forces
F_{x0}, F_{y0}	N	Initial conditions for the longitudinal and lateral forces
F_z	N	Vertical force
M_z	N m	Vertical moment
$\boldsymbol{p_\tau}$	N m^{-2}	Tangential shear stress vector
p_τ	N m^{-2}	Total tangential shear stress
p_x, p_y	N m^{-2}	Longitudinal and lateral shear stress
p_z	N m^{-2}	Vertical pressure

Displacements	Unit	Description
$\boldsymbol{u_\tau}$	m	Displacement vector of the bristle
u_x, u_y	m	Longitudinal and lateral displacement of the bristle
$\boldsymbol{u_{\tau 0}}$	m	Initial tangential displacement vector of the bristle (IC)
u_{x0}, u_{y0}	m	Initial longitudinal and lateral displacement (IC)
q	m	Travelled distance
$\boldsymbol{x}$	m	Coordinate vector

x, y	m	Longitudinal and lateral coordinates

Speeds	**Unit**	**Description**
V	$\mathrm{m\,s^{-1}}$	Rolling speed
$\boldsymbol{v}_{\partial\mathscr{C}}$	$\mathrm{m\,s^{-1}}$	Velocity of the contact patch boundary
$\bar{\boldsymbol{v}}_{\partial\mathscr{C}}$	$\mathrm{m\,s^{-1}}$	Nondimensional velocity of the contact patch boundary
$\boldsymbol{v}_{\boldsymbol{\tau}}$	$\mathrm{m\,s^{-1}}$	Tangential velocity field
$\bar{\boldsymbol{v}}_{\boldsymbol{\tau}}$	$\mathrm{m\,s^{-1}}$	Nondimensional tangential velocity field
v_x, v_y	$\mathrm{m\,s^{-1}}$	Longitudinal and lateral components of the velocity field

Slip Parameters	**Unit**	**Description**
$\boldsymbol{s}$	$\mathrm{m\,s^{-1}}$	Slip vector
s_x, s_y	$\mathrm{m\,s^{-1}}$	Longitudinal and lateral slips
$\boldsymbol{\xi}$	-	Creepage vector
ξ	-	Total creepage
ξ_x, ξ_y	-	Longitudinal and lateral creepages
ξ^{cr}	-	Critical creepage
$\tilde{\boldsymbol{\xi}}$	-	Modified creepage vector
$\tilde{\xi}$	-	Total modified creepage
$\tilde{\xi}_x, \tilde{\xi}_y$	-	Modified longitudinal and lateral creepages
$\tilde{\xi}^{\mathrm{cr}}$	-	Total modified creepage
ϕ	$\mathrm{m^{-1}}$	Critical modified creepage

Matrices and Tensors	**Unit**	**Description**
$\mathbf{A}_{\phi}$	$\mathrm{m^{-1}}$	Spin tensor
$\boldsymbol{\Phi}_{\boldsymbol{\tau}}$	-	State transition matrix

Geometric Parameters	**Unit**	**Description**
$A_{\mathscr{C}}$	$\mathrm{m^2}$	Contact patch area
a, b	m	Contact patch semilength and semiwidth
$\boldsymbol{\Lambda}_{\boldsymbol{\xi}}$	m	Matrix of tangential relaxation lengths
$\boldsymbol{\Lambda}_{\phi}$	m	Matrix of creepage relaxation lengths
$\boldsymbol{\Lambda}_{M\boldsymbol{\xi}}$	m	Matrix of rotational relaxation lengths
$\lambda_{x\xi_x}, \lambda_{y\xi_y}$	m	Longitudinal and lateral relaxation length
$\lambda_{x\xi_y}, \lambda_{y\xi_x}$	m	Cross relaxation lengths
$\lambda_{x\phi}, \lambda_{y\phi}$	m	Longitudinal and lateral spin relaxation lengths
$\lambda_{M\phi}$	m	Rotational spin relaxation length

Material Parameters	**Unit**	**Description**
G	$\mathrm{N\,m^2}$	Modulus of rigidity
ν	-	Poisson ratio

Stiffnesses and Compliances	**Unit**	**Description**
$\mathbf{C}_{\boldsymbol{\tau}}$	$\mathrm{N, N\,m, N\,m^2}$	Matrix of creep coefficients
C_{11}, C_{22}	N	Longitudinal and lateral creep coefficients
C_{23}	$\mathrm{N\,m}$	Cross creep coefficient
C_{33}	$\mathrm{N\,m^2}$	Rotational creep coefficient
$\mathbf{C}'_{\boldsymbol{\xi}}$	N	Matrix of modified creep coefficients
C'_{ξ_x}, C'_{ξ_y}	N	Modified longitudinal and lateral creep coefficients
$\mathbf{L}_{\boldsymbol{\tau}}$	$\mathrm{m^3\,N^{-1}}$	Matrix of tangential flexibilities
L_x, L_y	$\mathrm{m^3\,N^{-1}}$	Longitudinal and lateral flexibilities
$\mathbf{L}'_{\boldsymbol{F}}$	$\mathrm{m\,N^{-1}}$	Matrix of generalised tangential flexibilities

$\mathbf{L}'_M$	N^{-1}	Matrix of generalised rotational flexibilities
$\mathbf{L}'_{\phi F}$	N^{-1}	Matrix of generalised spin flexibilities
$\mathbf{L}'_{\phi M}$	$\mathrm{m\,N}^{-1}$	Rotational spin flexibility

Friction Parameters	Unit	Description
μ	-	Friction coefficient

Functions and Operators	Unit	Description
$\nabla_{\boldsymbol{\tau}}$	m^{-1}	Tangential gradient
$\nabla_{\tilde{\boldsymbol{\tau}}}$	m^{-1}	Transformed tangential gradient
$\check{\boldsymbol{\xi}}(\cdot,\cdot),\ \check{\phi}(\cdot,\cdot)$	-, m^{-1}	Slip functions
$\hat{\boldsymbol{\xi}}(\cdot,\cdot),\ \hat{\phi}(\cdot,\cdot)$	-, m^{-1}	Creepage functions

Sets	Unit	Description
$\mathscr{C}$	m^2	Contact patch
$\mathring{\mathscr{C}}$	m^2	Interior of $\mathscr{C}$
$\partial\mathscr{C}$	m	Boundary of $\mathscr{C}$
$\tilde{\mathscr{C}}$	m^2	Transformed contact patch
$\mathring{\tilde{\mathscr{C}}}$	m^2	Interior of $\tilde{\mathscr{C}}$
$\partial\tilde{\mathscr{C}}$	m	Boundary of $\tilde{\mathscr{C}}$
$\mathscr{L}$	m	Leading edge
$\tilde{\mathscr{L}}$	m	Transformed leading edge
$\mathscr{N}$	m	Neutral edge
$\tilde{\mathscr{N}}$	m	Transformed neutral edge
$\mathscr{T}$	m	Trailing edge
$\tilde{\mathscr{T}}$	m	Transformed trailing edge
$\mathbb{R}_{\geq 0}$	-	Set of positive real numbers (including 0)
$\mathbb{R}_{> 0}$	-	Set of strictly positive real numbers (excluding 0)

References

[1] Goryacheva IG, Rajeev PT, Farris TN. Wear in partial slip contact. J. Trib. 123(4): 848-856 (2001). Available from: https://doi.org/10.1016/j.wear.2010.02.018.

[2] Goryacheva IG, Torskaya EV. Modeling of fatigue wear of a two-layered elastic half-space in contact with periodic system of indenters, Wear 268(11-12):1417-1422 (2010). Available from: https://doi.org/10.1016/j.wear.2010.02.018.

[3] Zakharov SM, Goryacheva IG. Rolling contact fatigue defects in freight car wheels, Wear 258(7-8):1142-1147 (2005). Available from: https://doi.org/10.1016/j.wear.2004.03.062.

[4] Kalker JJ. On the rolling contact of two elastic bodies in the presence of dry friction. Dissertation, TH Delft, Delft (1967).

[5] Kalker JJ. Transient Phenomena in Two Elastic Cylinders Rolling Over Each Other With Dry Friction. Journal of Applied Mechanics. 1970, 37(3): 677-688. Available from: https://doi.org/10.1115/1.3408597.

[6] Kalker JJ. Transient rolling contact phenomena. ASLE Trans. 1971;14(3):177-184. Available from: https://doi.org/10.1080/05698197108983240.

[7] Kalker JJ. Three-Dimensional Elastic Bodies in Rolling Contact. Springer: Dordrecht; 1990. Available from: https://doi.org/10.1007/978-94-015-7889-9.

[8] Johnson KL. Contact Mechanics. Cambridge University Press; 1985. Available from: https://doi.org/10.1017/CBO9781139171731.

[9] Goryacheva IG. Contact Mechanics in Tribology. Springer Science & Business Media. 1998.

[10] Barber JR. Contact Mechanics. Springer International Publishing; 2018. Available from: https://doi.org/10.1007/978-3-319-70939-0.

[11] Vollebregt EAH. User guide for CONTACT, Vollebregt & Kalker's rolling and sliding contact model. Techical report TR09-03, version 13.

[12] Vollebregt EAH, Wilders P. FASTSIM2: a second-order accurate frictional rolling contact algorithm. Computational Mechanics 47 (1), 105-116; 2011. Available from: https://doi.org/10.1007/s00466-010-0536-7.

[13] Vollebregt EAH, Iwnicki SD, Xie G, Shackelton P. Assessing the accuracy of different simplified frictional rolling contact algorithms. Vehicle System Dynamics 50 (1), 1-17; 2012. Available from: https://doi.org/10.1080/00423114.2011.552618.

[14] Vollebregt EAH. Numerical modeling of measured railway creep versus creep-force curves with CONTACT. Wear 314(1-2), 87-95; 2014. Available from: https://doi.org/10.1016/j.wear.2013.11.030.

[15] Nielsen JB. New developments in the theory of wheel/rail contact mechanics. PhD thesis. University of Denmark; 1998. Available from: https://orbit.dtu.dk/en/publications/new-developments-in-the-theory-of-wheelrail-contact-mechanics.

[16] Dahlberg J, Alfredsson B. Transient rolling of cylindrical contacts with constant and linearly increasing applied slip. Wear. 2009;266(1-2):316-326. Available from: https://doi.org/10.1016/j.wear.2008.07.008.

[17] Kalker JJ. Simplified theory of rolling contact. Delft Progress Report, Series C, Mechanical and Aeronautical Engineering and Shipbuilding (Delft University Press, Delft, 1973), pp. 1–10.

[18] Kalker JJ. railway wheel and automotive tyre. Vehicle Syst. Dyn. 1979;5(15):255-269.

[19] Knothe K, Groß-Thebing A. Short wavelength rail corrugation and non-steady-state contact mechanics. Vehicle Syst. Dyn. 2008;46(1-2):49-66. Available from: https://doi.org/10.1080/00423110701590180.

[20] Alonso A, Giménez JG. Non-steady state modelling of wheel-rail contact problem for the dynamic simulation of railway vehicles. Vehicle Syst. Dyn. 2008;46(3):179-196. Available from: https://doi.org/10.1080/00423110701248011.

[21] Guiral A, Alonso A, Baeza L,Giménez JG. Non-steady state modelling of wheel–rail contact problem, Vehicle System Dynamics. 2013;51(1):91-108. Available from: https://doi.org/10.1080/00423114.2012.713499.

[22] Ciavarella M, Barber J. Influence of longitudinal creepage and wheel inertia on short-pitch corrugation: A resonance-free mechanism to explain the roaring rail phenomenon. Proceedings of the Institution of Mechanical Engineers, Part J: Journal of Engineering Tribology 222(3); 2008. Available from: https://doi.org/10.1243/13506501JET373.

[23] Afferrante L, Ciavarella M. Short-pitch rail corrugation: A possible resonance-free regime as a step forward to explain the "enigma"? Wear 266(9-10); 2008. Available from: https://doi.org/10.1016/j.wear.2008.12.003.

[24] Afferrante L, Ciavarella M. Short pitch corrugation of railway tracks with wooden or concrete sleepers: An enigma solved? Tribology International 43(3); 2010. Available from: https://doi.org/10.1016/j.triboint.2009.09.010.

[25] Guiggiani M. The Science of Vehicle Dynamics, 2nd ed. Cham(Switzerland): Springer International; 2018.

[26] Pacejka HB. Tire and vehicle dynamics. 3rd ed. Amsterdam: Elsevier/BH; 2012.

[27] Frendo F, Bucchi F. "Brush model" for the analysis of flat belt transmissions in steady-state conditions. Mechanism and Machine Theory. 2020. 143. Available from https://doi.org/10.1016/j.mechmachtheory.2019.103653.

[28] Frendo F, Bucchi F. Enhanced brush model for the mechanics of power transmission in flat belt drives under steady–state conditions: Effect of belt elasticity. Mechanism and Machine Theory. 2020. 153. Available from: https://doi.org/10.1016/j.mechmachtheory.2020.103998.

[29] Bucchi F, Frendo F. Validation of the brush model for the analysis of flat belt transmissions in steady-state conditions by finite element simulation. Mechanism and Machine Theory. 2022. 167. Available from: https://doi.org/10.1016/j.mechmachtheory.2021.104556.

[30] Al-Bender F, De Moerlooze K. A Model of the Transient Behavior of Tractive Rolling Contacts. Advances in Tribology, Hindawi Publishing Corporation; 2008. Available from: https://doi.org/10.1155/2008/214894.

[31] Romano L, Bruzelius F, Jacobson B. Unsteady-state brush theory. Vehicle Syst. Dyn. 2020; pages 1-29. Available from: https://doi.org/10.1080/00423114.2020.1774625.

[32] Romano L. Advanced Brush Tyre Modelling. SpringerBriefs in Applied Sciences. Springer, Cham (2022). Available from: https://doi.org/10.1007/978-3-030-98435-9.

[33] Romano L, Bruzelius F Jacobson B. Brush tyre models for large camber angles and steering speeds. Vehicle System Dynamics, 60:4, 1341-1392. Available from: https://doi.org/10.1080/00423114.

`2020.1854320`.

[34] Romano L, Timpone F, Bruzelius F, Jacobson B. Analytical results in transient brush tyre models: theory for large camber angles and classic solutions with limited friction. Meccanica 57, 165-191 (2022). Available from: `http://dx.doi.org/10.1007/s11012-021-01422-3`.

[35] Romano L, Timpone F, Bruzelius F, Jacobson B. Rolling, tilting and spinning spherical wheels: analytical results using the brush theory. Mechanism and Machine Theory 173 (2022). Available from: `https://doi.org/10.1016/j.mechmachtheory.2022.104836`.

[36] Knothe K, Stichel S. Rail Vehicle Dynamics. Springer Cham; 2017. Available from: `https://doi.org/10.1007/978-3-319-45376-7`.

[37] Voltr P, Lata M. Transient problems in rolling contact of wheel and rail. 9th International Conference on Railway Bogies and Running Gears. Budapest, Hungary.

[38] Voltr P. Calculation of locomotive traction force in transient rolling contact. Applied and Computational Mechanics 11(69-80); 2016.

[39] Romano L, Bruzelius F, Hjort M, Jacobson B. Development and analysis of the two-regime transient tyre model for combined slip. Vehicle Syst. Dyn. 2022.

[40] Carter FW. On the action of a locomotive driving wheel.Proceedings of the Royal Society of London. Series A, containing papers ofa mathematical and physical character, 112(760), 151-157; 1926. Available from: `https://royalsocietypublishing.org/doi/10.1098/rspa.1926.0100`.

[41] Hobbs AEW. A Survey on Creep. Technical Note TN DYN 52, British Rail Research, Derby (1967) (reprinted 1976).

[42] Shen ZY, Hedrick JK, Elkins JA. A comparison of alternative creep-force models for rail vehicle dynamic analysis, in The Dynamics of Vehicles on Roads and Tracks. Proceedings of the 8th IAVSD Symposium held at MIT Cambridge/MA, August 15–19, 1983, ed. by J.K. Hedrick (Swets and Zeitlinger, Lisse, 1984), pp. 591–60.

[43] Evans LC. Partial differential equations. 2nd ed. American Mathematical Society; 1996.

[44] Ockendon JR, Howison S, Lacey A, Movchan A. Applied partial differential equations. Oxford University Press; 2003.

[45] Larsson S, Thomee V. Partial Differential Equations with Numerical Methods. 1st ed. Springer, Berlin, Heidelberg. 2009. Available from: `https://doi.org/10.1007/978-3-540-88706-5`.

[46] Persson BNJ. Theory of rubber friction and contact mechanics. The Journal of Chemical Physics 2001;115(8):3840-3861. Available from: `https://doi.org/10.1063/1.1388626`.

[47] Persson BNJ, Albohr O, Tartaglino U, Volokitin AI, Tosatti E. On the nature of surface roughness with application to contact mechanics, sealing, rubber friction and adhesion. Journal of Physics: Condensed Matter 20004;17(1):R1-R62.

[48] Persson BNJ. Contact mechanics for randomly rough surfaces. Surface Science Reports. 2006;61(4):201-227. Available from: `https://doi.org/10.1016/j.surfrep.2006.04.001`.

[49] Goryacheva I, Sadeghi F. Contact characteristics of a rolling/sliding cylinder and a viscoelastic layer bonded to an elastic substrate, Wear 184(2):125-132 (1995). Available from: `https://doi.org/10.1016/0043-1648(94)06561-6`.

[50] Carbone G, Putignano C. A novel methodology to predict sliding and rolling friction of viscoelastic materials: Theory and experiments, J. Mech. Phys. Solids 61(8):1822-1834 (2013). Available from: `https://doi.org/10.1016/j.jmps.2013.03.005`

[51] Santeramo M, Putignano C, Vorlaufer G, et al. Viscoelastic steady-state rolling contacts: A generalized boundary element formulation for conformal and non-conformal geometries, J. Mech. Phys. Solids 171 (2023). Available from: `https://doi.org/10.1016/j.jmps.2022.105129`.

[52] Kalker JJ. Variational Principles of Contact Elastostatics. J. Inst. Maths. Applics. 1997;20:199-219.

[53] Kalker JJ. A minimum principle for the law of dry friction with application to elastic cylinders in rolling contact, Transactions ASME, Journal of Applied Mechanics, 38, part 1: 875-880, fundamentals,application to steady-state rolling. part 2: 881-887.Application to non-steady rolling elastic cylinders.

[54] Hertz H. Über die Berührung fester, elastischer Körper. (On the contact of solid elastic bodies). Journal für die reine und angewandte Mathematik 92, 156–171 (1882).

[55] Hertz H. Über die Berührung fester elastischer Körper (On the contact of solid elastic bodies), in Heinrich Hertz, Collected Works. Band 1, Leipzig (1895), pp. 155–173.

[56] Vollebregt E, Voltr P. Improved accuracy for FASTSIM using one or three flexibility values. Vehicle System Dynamics 61(1):309-317 (2023).

[57] Crippa G, Donadello C, Spinolo LV. Initial–boundary value problems for continuity equations with BV coefficients, Journal de Mathématiques Pures et Appliquées 102(1):79-98 (2014).

[58] Crippa G, Donadello C, Spinolo LV. A note on the initial-boundary value problem for the continuity equations with rough coefficients, Hyperbolic problems: theory, numerics, applications, 8. pp. 957-966.

[59] Bardos C. Problèmes aux limites pour les équations aux dérivées partielles du premier ordre à coefficients réels, théorèmes d'approximation application à l'équation de transport, Ann. Sci. Éc. Norm. Super. (4), 3 (1970), pp. 185-233.

[60] Matoušek J. On directional convexity. Discrete Comput Geom 25, 389–403 (2001). Available from: https://doi.org/10.1007/s004540010069.

[61] Kalker JJ. Survey of wheel-rail rolling contact theory. Vehicle Syst Dyn. 1997;8(4):317-358. Available from: https://doi.org/10.1080/00423117908968610.

[62] Kreiss HO, Lorenz J. Initial-Boundary Value Problems and the Navier-Stokes Equations. Society for Industrial and Applied Mathematics, 2004. Available from: https://epubs.siam.org/doi/abs/10.1137/1.9780898719130.

[63] Gustafsson B, Kreiss HO, Oliger J. Time-Dependent Problems and Difference Methods, 2nd ed. Wiley, Pure and Applied Mathematics (2013).

[64] Gustafsson B. High Order Difference Methods for Time Dependent PDE. 1st ed. Springer (2007).

[65] Ern A, Guermond J-L. Theory and Practice of Finite Elements, 1st ed. Springer New York (2004). Available from: https://doi.org/10.1007/978-1-4757-4355-5.

[66] Vollebregt EAH. Updates on the rocking phenomenon. The Dynamics of Vehicles on Roads and Tracks, 605-611 (2017).

[67] Polach O. Creep forces in simulations of traction vehicles running on adhesion limit. Wear 258:992-1000 (2005).

[68] Spiryagin M, Polach O, Cole C. Creep force modelling for rail traction vehicles based on the Fastsim algorithm. Veh Syst Dyn 51:1765-1783 (2013).

[69] Six K, AMeierhofer A, Müller G, Dietmaier P. Physical processes in wheel-rail contact and its implications on vehicle-track interaction, Vehicle System Dynamics 53(5)635:650 (2015).

[70] Khalil HK. Nonlinear Systems. 3rd ed. Prentice Hall, Upper Saddle River; 2002.

[71] Rugh WJ. Linear System Theory. 2nd ed. Johns Hopkins University; 2007.

[72] Piotrowski J, Liu B, Bruni S. The Kalker book of tables for non-Hertzian contact of wheel and rail, Vehicle System Dynamics 55(6):875-901 (2017). Available from: http://dx.doi.org/10.1080/00423114.2017.1291980.

[73] Vollebregt EAH. Comments on 'the Kalker book of tables for non-Hertzian contact of wheel and rail', Vehicle System Dynamics 56(9):1451-1459 (2018).

[74] Liu B, Fu B, Bruni S. Generalisation of the linear theory of rolling contact to a single double-elliptic contact region and its application to solve non-Hertzian contact problems using extended FASTSIM, Vehicle System Dynamics, pp. 1-19 (2022). Available from: https://doi.org/10.1080/00423114.2022.2113808.

[75] Johnson KL. The effect of a tangential contact force upon the rolling motion of an elastic sphere on a plane. J. Appl. Mech. 25, 339–346 (1958). Available from: https://doi.org/10.1115/1.4011823.

[76] Johnson KL. The effect of spin upon the rolling motion of an elastic sphere on a plane. J. Appl. Mech. 25, 332–338 (1958). Available from: https://doi.org/10.1115/1.4011822.

[77] Vermeulen J, Johnson KL. Contact of nonspherical elastic bodies transmitting tangential forces. J. Appl. Mech. 31, 338–340 (1964). Available from: https://doi.org/10.1115/1.3629610.

[78] He C, Hsiao L. Two-Dimensional Euler Equations in a Time Dependent Domain. Journal of Differential Equations 163(2):265-291 (2000). Available from: https://doi.org/10.1006/jdeq.1999.3702.

[79] Truesdell C, Toupin RA. The classical field theories. In Flügge S, editor, Handbuch der Physik, vol. 3/1, page 226. Springer-Verag: Berlin; 1960.

[80] Truesdell C, Rajagopal KR. An Introduction to the Mechanics of Fluids. Birkhäuser Boston 2000. Available from: https://doi.org/10.1007/978-0-8176-4846-6.

A   Time-varying contact patch

The present appendix illustrates a simple method to deal with a time-varying contact patch. The approach is restricted for simplicity to the simplified theory discussed in Sect. 4, particularly concerning no-slip conditions; the generalisation to the other theories considered in the paper is however straightforward. Furthermore, the travelled distance q is directly adopted as independent time-like variable in place of the time t to lighten the notation. More specifically, to cope with the fact that the domain $\mathring{\mathscr{C}}_\infty \triangleq$

$\cup_{q\in\mathbb{R}}\mathring{\mathscr{C}}(q)\times\{q\}$ is noncylindrical, the following Assumption[9] is introduced [78].

Assumption A.1. *There exists a cylindrical domain $\mathring{\tilde{\mathscr{C}}}_\infty \triangleq \mathring{\tilde{\mathscr{C}}}\times\mathbb{R}$ and a level-preserving C^∞-diffeomorphism $\boldsymbol{\Phi} : (\tilde{\boldsymbol{x}},\tilde{q}) = \boldsymbol{\Phi}(\boldsymbol{x},q) = [\boldsymbol{\Phi_x}(\boldsymbol{x},q)^\mathrm{T}\ q]^\mathrm{T} = [\Phi_x(\boldsymbol{x},q)\ \Phi_y(\boldsymbol{x},q)\ q]^\mathrm{T}$ from $\mathscr{C}_\infty \mapsto \tilde{\mathscr{C}}_\infty$, with inverse denoted by $\boldsymbol{\Xi} : (\boldsymbol{x},q) = \boldsymbol{\Xi}(\tilde{\boldsymbol{x}},\tilde{q}) = [\boldsymbol{\Xi_{\tilde{x}}}(\tilde{\boldsymbol{x}},\tilde{q})^\mathrm{T}\ \tilde{q}]^\mathrm{T} = [\Xi_{\tilde{x}}(\tilde{\boldsymbol{x}},\tilde{q})\ \Xi_{\tilde{y}}(\tilde{\boldsymbol{x}},\tilde{q})\ \tilde{q}]^\mathrm{T}$.*

According to the above Assumption A.1, by defining

$$\tilde{\boldsymbol{u}}_{\boldsymbol{\tau}}(\tilde{\boldsymbol{x}},\tilde{q}) = \boldsymbol{u}_{\boldsymbol{\tau}}(\boldsymbol{x},q)\bigg|_{(\boldsymbol{x},q)=\boldsymbol{\Xi}(\tilde{\boldsymbol{x}},\tilde{q})}, \tag{83}$$

$$\tilde{\boldsymbol{u}}_{\boldsymbol{\tau}0}(\tilde{\boldsymbol{x}}) = \boldsymbol{u}_{\boldsymbol{\tau}0}(\boldsymbol{x})\bigg|_{(\boldsymbol{x},0)=\boldsymbol{\Xi}(\tilde{\boldsymbol{x}},0)},$$

$$\tilde{\boldsymbol{v}}_{\boldsymbol{\tau}}(\tilde{\boldsymbol{x}},\tilde{q}) = \left(\left(\bar{\boldsymbol{v}}_{\boldsymbol{\tau}}(\boldsymbol{x},q)\cdot\nabla_{\boldsymbol{\tau}}\right)\boldsymbol{\Phi_x}(\boldsymbol{x},q) + \frac{\partial\boldsymbol{\Phi_x}(\boldsymbol{x},q)}{\partial q}\right)\bigg|_{(\boldsymbol{x},q)=\boldsymbol{\Xi}(\tilde{\boldsymbol{x}},\tilde{q})}, \tag{84}$$

the original problem described by Eq. (20) becomes

$$\frac{\partial\tilde{\boldsymbol{u}}_{\boldsymbol{\tau}}(\tilde{\boldsymbol{x}},\tilde{q})}{\partial\tilde{q}} + \tilde{\boldsymbol{v}}_{\boldsymbol{\tau}}(\tilde{\boldsymbol{x}},\tilde{q})\cdot\nabla_{\tilde{\boldsymbol{\tau}}}\tilde{\boldsymbol{u}}_{\boldsymbol{\tau}}(\boldsymbol{x},q) = -\tilde{\boldsymbol{\xi}}(\tilde{q}) - \mathbf{A}_{\tilde{\phi}}(\tilde{q})\boldsymbol{\Xi_{\tilde{x}}}(\tilde{\boldsymbol{x}},\tilde{q}), \qquad (\tilde{\boldsymbol{x}},\tilde{q})\in\mathring{\tilde{\mathscr{C}}}\times\mathbb{R}_{>0}, \tag{85}$$

where $\nabla_{\tilde{\boldsymbol{\tau}}} \triangleq [\partial/\partial\tilde{x}\ \partial/\partial\tilde{y}]^\mathrm{T}$ and clearly $\tilde{\boldsymbol{\xi}}(\tilde{q}) = [\tilde{\xi}_x(\tilde{q})\ \tilde{\xi}_y(\tilde{q})]^\mathrm{T} \equiv \boldsymbol{\xi}(q)$ and $\tilde{\phi}(\tilde{q}) \equiv \phi(q)$. The new PDEs (85) are supplemented with the following BC and IC:

BC: $\qquad\qquad\tilde{\boldsymbol{u}}_{\boldsymbol{\tau}}(\tilde{\boldsymbol{x}},\tilde{q}) = \boldsymbol{0}, \qquad\qquad (\tilde{\boldsymbol{x}},\tilde{q})\in\tilde{\mathscr{L}}\times\mathbb{R}_{>0}, \tag{86}$

IC: $\qquad\qquad\tilde{\boldsymbol{u}}_{\boldsymbol{\tau}}(\tilde{\boldsymbol{x}},0) = \tilde{\boldsymbol{u}}_{\boldsymbol{\tau}0}(\tilde{\boldsymbol{x}}), \qquad\qquad \tilde{\boldsymbol{x}}\in\mathring{\tilde{\mathscr{C}}}, \tag{87}$

in which the new definition for the leading, neutral, and trailing edges read

$$\tilde{\mathscr{L}} \triangleq \left\{\tilde{\boldsymbol{x}}\in\partial\tilde{\mathscr{C}}\ \bigg|\ \tilde{\boldsymbol{v}}_{\boldsymbol{\tau}}(\tilde{\boldsymbol{x}},\tilde{q})\cdot\hat{\boldsymbol{n}}_{\partial\tilde{\mathscr{C}}}(\tilde{\boldsymbol{x}}) < 0\right\}, \tag{88a}$$

$$\tilde{\mathscr{N}} \triangleq \left\{\tilde{\boldsymbol{x}}\in\partial\tilde{\mathscr{C}}\ \bigg|\ \tilde{\boldsymbol{v}}_{\boldsymbol{\tau}}(\tilde{\boldsymbol{x}},\tilde{q})\cdot\hat{\boldsymbol{n}}_{\partial\tilde{\mathscr{C}}}(\tilde{\boldsymbol{x}}) = 0\right\}, \tag{88b}$$

$$\tilde{\mathscr{T}} \triangleq \left\{\tilde{\boldsymbol{x}}\in\partial\tilde{\mathscr{C}}\ \bigg|\ \tilde{\boldsymbol{v}}_{\boldsymbol{\tau}}(\tilde{\boldsymbol{x}},\tilde{q})\cdot\hat{\boldsymbol{n}}_{\partial\tilde{\mathscr{C}}}(\tilde{\boldsymbol{x}}) > 0\right\}, \tag{88c}$$

being $\hat{\boldsymbol{n}}_{\partial\tilde{\mathscr{C}}}(\tilde{\boldsymbol{x}})$ the unit normal to $\partial\tilde{\mathscr{C}}$. The equivalence between the original BC (24a) and that for the transformed system in Eq. (88a) may be derived starting from some basic considerations concerning differential geometry. Indeed, describing the boundary of the time-varying domain in implicit form as $\partial\mathscr{C}(q) = \{\boldsymbol{x}\in\mathbb{R}^2\ |\ \gamma_{\partial\mathscr{C}}(\boldsymbol{x},q) = 0\}$, for some function $\gamma_{\partial\mathscr{C}}(\cdot,\cdot)$, the outward-pointing unit normal $\hat{\boldsymbol{n}}_{\partial\mathscr{C}}(\boldsymbol{x},q)$ and a representation of the nondimensional boundary velocity $\bar{\boldsymbol{v}}_{\partial\mathscr{C}}(\boldsymbol{x},q)$ that is oriented as the unit normal are given respectively by [79, 80]

$$\hat{\boldsymbol{n}}_{\partial\mathscr{C}}(\boldsymbol{x},q) = \pm\frac{\nabla_{\boldsymbol{\tau}}\gamma_{\partial\mathscr{C}}(\boldsymbol{x},q)}{\left\|\nabla_{\boldsymbol{\tau}}\gamma_{\partial\mathscr{C}}(\boldsymbol{x},q)\right\|}, \tag{89a}$$

$$\bar{\boldsymbol{v}}_{\partial\mathscr{C}}(\boldsymbol{x},q) = -\frac{\nabla_{\boldsymbol{\tau}}\gamma_{\partial\mathscr{C}}(\boldsymbol{x},q)}{\left\|\nabla_{\boldsymbol{\tau}}\gamma_{\partial\mathscr{C}}(\boldsymbol{x},q)\right\|^2}\frac{\partial\gamma_{\partial\mathscr{C}}(\boldsymbol{x},q)}{\partial q}\,. \tag{89b}$$

---

[9]Some of the requirements in Assumption A.1 are rather strict, and may eventually be relaxed; however, they are kept in this paper for simplicity and in order to allocate the smoothness requirements directly on the original velocity field.

Hence, departing from the relationships in Eqs. (89), it may be inferred that

$$
\begin{aligned}
\left[\bar{\boldsymbol{v}}_{\boldsymbol{\tau}}(\boldsymbol{x}, q) - \bar{\boldsymbol{v}}_{\partial\mathscr{C}}(\boldsymbol{x}, q)\right] \cdot \hat{\boldsymbol{n}}_{\partial\mathscr{C}}(\boldsymbol{x}, q) &= \pm \frac{\nabla_{\boldsymbol{\tau}}\gamma_{\partial\mathscr{C}}(\boldsymbol{x}, q)}{\left\|\nabla_{\boldsymbol{\tau}}\gamma_{\partial\mathscr{C}}(\boldsymbol{x}, q)\right\|} \cdot \left(\bar{\boldsymbol{v}}_{\boldsymbol{\tau}}(\boldsymbol{x}, q) + \frac{\nabla_{\boldsymbol{\tau}}\gamma_{\partial\mathscr{C}}(\boldsymbol{x}, q)}{\left\|\nabla_{\boldsymbol{\tau}}\gamma_{\partial\mathscr{C}}(\boldsymbol{x}, q)\right\|^2} \frac{\partial\gamma_{\partial\mathscr{C}}(\boldsymbol{x}, q)}{\partial q}\right) \\
&= \pm \frac{1}{\left\|\nabla_{\boldsymbol{\tau}}\gamma_{\partial\mathscr{C}}(\boldsymbol{x}, q)\right\|} \cdot \left(\nabla_{\boldsymbol{\tau}}\gamma_{\partial\mathscr{C}}(\boldsymbol{x}, q) \cdot \bar{\boldsymbol{v}}_{\boldsymbol{\tau}}(\boldsymbol{x}, q) + \frac{\partial\gamma_{\partial\mathscr{C}}(\boldsymbol{x}, q)}{\partial q}\right) \\
&= \pm \frac{1}{\left\|\nabla_{\boldsymbol{\tau}}\gamma_{\partial\mathscr{C}}(\boldsymbol{x}, q)\right\|} \cdot \left(\nabla_{\boldsymbol{\tau}}\gamma_{\partial\mathscr{C}}(\boldsymbol{x}, q) \cdot \bar{\boldsymbol{v}}_{\boldsymbol{\tau}}(\boldsymbol{x}, q) + \nabla_{\tilde{\boldsymbol{\tau}}}\gamma_{\partial\mathscr{C}}(\boldsymbol{x}, q) \cdot \frac{\partial\boldsymbol{\Phi}_{\boldsymbol{x}}(\boldsymbol{x}, q)}{\partial q}\right) \\
&= \pm \frac{\nabla_{\tilde{\boldsymbol{\tau}}}\gamma_{\partial\mathscr{C}}(\boldsymbol{x}, q)}{\left\|\nabla_{\boldsymbol{\tau}}\gamma_{\partial\mathscr{C}}(\boldsymbol{x}, q)\right\|} \cdot \left(\left(\bar{\boldsymbol{v}}_{\boldsymbol{\tau}}(\boldsymbol{x}, q) \cdot \nabla_{\boldsymbol{\tau}}\right)\boldsymbol{\Phi}_{\boldsymbol{x}}(\boldsymbol{x}, q) + \frac{\partial\boldsymbol{\Phi}_{\boldsymbol{x}}(\boldsymbol{x}, q)}{\partial q}\right) \\
&= \frac{\left\|\nabla_{\tilde{\boldsymbol{\tau}}}\gamma_{\partial\mathscr{C}}(\boldsymbol{x}, q)\right\|}{\left\|\nabla_{\boldsymbol{\tau}}\gamma_{\partial\mathscr{C}}(\boldsymbol{x}, q)\right\|} \left.\tilde{\boldsymbol{v}}_{\boldsymbol{\tau}}(\tilde{\boldsymbol{x}}, \tilde{q}) \cdot \hat{\boldsymbol{n}}_{\partial\tilde{\mathscr{C}}}(\tilde{\boldsymbol{x}})\right|_{(\tilde{\boldsymbol{x}}, \tilde{q})=\boldsymbol{\Phi}(\boldsymbol{x}, q)},
\end{aligned}
$$
(90)

which establishes the equivalence between the BCs (24a) and (88a). It is worth mentioning that, according to the alternative formulation of the problem described by Eqs. (85), the BC (88a) is still noncharacteristic [43, 45].

The resulting system of PDEs (85), equipped with BC and IC given respectively by (86) and (87), has exactly the same structure as that of Eqs. (20), (22) and (23) when the contact patch is fixed, implying that, under the same assumptions on the domain $\mathscr{C}$ and nondimensional velocity $\tilde{\boldsymbol{v}}_{\boldsymbol{\tau}}(\tilde{\boldsymbol{x}}, \tilde{q})$, a unique generalised solution $\tilde{\boldsymbol{u}}_{\boldsymbol{\tau}}(\tilde{\boldsymbol{x}}, \tilde{q}) \in L^\infty(\overset{\circ}{\tilde{\mathscr{C}}} \times (0, \tilde{Q}); \mathbb{R}^2)$ is guaranteed to exist. Due to the diffeomorphisms $\boldsymbol{\Phi}: (\tilde{\boldsymbol{x}}, \tilde{q}) = \boldsymbol{\Phi}(\boldsymbol{x}, q)$ and $\boldsymbol{\Xi}: (\boldsymbol{x}, q) = \boldsymbol{\Xi}(\tilde{\boldsymbol{x}}, \tilde{q})$, the solution $\boldsymbol{u}_{\boldsymbol{\tau}}(\boldsymbol{x}, q)$ to the original problem is also unique, owing to Assumption A.1.

The two following examples clarify the proposed method concerning the cases of line contact and elliptical contact patch, respectively.

Example A.1 (Line contact). *Consider line contact conditions, i.e., $\mathscr{C}(q) = \{x \in \mathbb{R} \mid \gamma_{\partial\mathscr{C}}(x, q) \leq 0\}$, $\partial\mathscr{C}(q) = \{x \in \mathbb{R} \mid \gamma_{\partial\mathscr{C}}(x, q) = 0\}$, with*

$$
\gamma_{\partial\mathscr{C}}(x, q) = \frac{|x|}{a(q)} - 1,
$$
(91)

and, e.g., $a(q) \in [a_{\min}, a_{\max}]$ with $a_{\min} > 0$. Assuming sufficient regularity for $a(q)$, the diffeomorphism $(\tilde{x}, \tilde{q}) = \boldsymbol{\Phi}(x, q) = [\Phi_x(x, q)\ q]^{\mathrm{T}}$ given by

$$
\boldsymbol{\Phi}(x, q) = \begin{bmatrix} \Phi_x(x, q) & q \end{bmatrix}^{\mathrm{T}} = \begin{bmatrix} \dfrac{x}{a(q)} & q \end{bmatrix}^{\mathrm{T}},
$$
(92)

with inverse mapping $(x, q) = \boldsymbol{\Xi}(\tilde{x}, \tilde{q}) = [\Xi_{\tilde{x}}(\tilde{x}, \tilde{q})\ \tilde{q}]^{\mathrm{T}}$ reading

$$
\boldsymbol{\Xi}(\tilde{x}, \tilde{q}) = \begin{bmatrix} \Xi_{\tilde{x}}(\tilde{x}, \tilde{q}) & \tilde{q} \end{bmatrix}^{\mathrm{T}} = \begin{bmatrix} a(\tilde{q})\tilde{x} & \tilde{q} \end{bmatrix}^{\mathrm{T}},
$$
(93)

maps Eq. (91) into

$$
\gamma_{\partial\tilde{\mathscr{C}}}(\tilde{x}) = \left.\gamma_{\partial\mathscr{C}}(x, q)\right|_{(x, q)=\boldsymbol{\Xi}(\tilde{x}, \tilde{q})} = |\tilde{x}| - 1,
$$
(94)

and consequently the original domain into $\tilde{\mathscr{C}} = \{\tilde{x} \in \mathbb{R} \mid \gamma_{\partial\tilde{\mathscr{C}}}(\tilde{x}) \leq 0\}$ with boundary $\partial\tilde{\mathscr{C}} = \{\tilde{x} \in \mathbb{R} \mid \gamma_{\partial\tilde{\mathscr{C}}}(\tilde{x}) = 0\}$. From Eqs. (84), (92) and (93), the scalar nondimensional transport velocity $\tilde{v}_{\boldsymbol{\tau}}(\tilde{x}, \tilde{q})$ may be deduced as

$$
\tilde{v}_{\boldsymbol{\tau}}(\tilde{x}, \tilde{q}) = -\frac{1}{a(\tilde{q})}\left(1 + \tilde{x}\,\frac{\partial a(\tilde{q})}{\partial\tilde{q}}\right).
$$
(95)

In the the previously adduced Example (A.1), the resulting scalar velocity field $\tilde{v}_{\boldsymbol{\tau}}(\tilde{x}, \tilde{q})$ was obviously only a function of the new longitudinal and time-like coordinates. For an elliptical contact patch, it may also vary with the transformed lateral coordinate, as illustrated in Example (A.2).

Example A.2 (Elliptical contact patch). *Consider an elliptical contact patch $\mathscr{C}(q) = \{\boldsymbol{x} \in \mathbb{R}^2 \mid \gamma_{\partial\mathscr{C}}(\boldsymbol{x}, q) \leq 0\}$ and boundary $\partial\mathscr{C}(q) = \{\boldsymbol{x} \in \mathbb{R}^2 \mid \gamma_{\partial\mathscr{C}}(\boldsymbol{x}, q) = 0\}$, with*

$$\gamma_{\partial\mathscr{C}}(\boldsymbol{x}, q) = \frac{x^2}{a^2(q)} + \frac{y^2}{b^2(q)} - 1, \tag{96}$$

and, e.g., $a(q) \in [a_{\min}, a_{\max}]$ ($a_{\min} > 0$), and $b(q) \in [b_{\min}, b_{\max}]$ ($b_{\min} > 0$). Assuming sufficient regularity for $a(q)$ and $b(q)$, the diffeomorphism $(\tilde{\boldsymbol{x}}, \tilde{q}) = \boldsymbol{\Phi}(\boldsymbol{x}, q) = [\Phi_x(x, q)\ \Phi_y(y, q)\ q]^{\mathrm{T}}$ given by

$$\boldsymbol{\Phi}(\boldsymbol{x}, q) = \begin{bmatrix} \Phi_x(x, q) & \Phi_y(y, q) & q \end{bmatrix}^{\mathrm{T}} = \begin{bmatrix} \dfrac{\tilde{a}}{a(q)}x & \dfrac{\tilde{b}}{b(q)}y & q \end{bmatrix}^{\mathrm{T}}, \tag{97}$$

with $\tilde{a}, \tilde{b} > 0$, and inverse mapping $(\boldsymbol{x}, q) = \boldsymbol{\Xi}(\tilde{\boldsymbol{x}}, \tilde{q}) = [\Xi_{\tilde{x}}(\tilde{x}, \tilde{q})\ \Xi_{\tilde{y}}(\tilde{y}, \tilde{q})\ \tilde{q}]^{\mathrm{T}}$ reading

$$\boldsymbol{\Xi}(\tilde{\boldsymbol{x}}, \tilde{q}) = \begin{bmatrix} \Xi_{\tilde{x}}(\tilde{x}, \tilde{q}) & \Xi_{\tilde{y}}(\tilde{y}, \tilde{q}) & \tilde{q} \end{bmatrix}^{\mathrm{T}} = \begin{bmatrix} \dfrac{a(\tilde{q})}{\tilde{a}}\tilde{x} & \dfrac{b(\tilde{q})}{\tilde{b}}\tilde{y} & \tilde{q} \end{bmatrix}^{\mathrm{T}}, \tag{98}$$

maps Eq. (96) into

$$\gamma_{\partial\tilde{\mathscr{C}}}(\tilde{\boldsymbol{x}}) = \gamma_{\partial\mathscr{C}}(\boldsymbol{x}, q)\bigg|_{(\boldsymbol{x}, q) = \boldsymbol{\Xi}(\tilde{\boldsymbol{x}}, \tilde{q})} = \frac{\tilde{x}^2}{\tilde{a}^2} + \frac{\tilde{y}^2}{\tilde{b}^2} - 1, \tag{99}$$

and consequently the original domain into $\tilde{\mathscr{C}} = \{\tilde{\boldsymbol{x}} \in \mathbb{R}^2 \mid \gamma_{\partial\tilde{\mathscr{C}}}(\tilde{\boldsymbol{x}}) \leq 0\}$ with constant boundary $\partial\tilde{\mathscr{C}} = \{\boldsymbol{x} \in \mathbb{R}^2 \mid \gamma_{\partial\tilde{\mathscr{C}}}(\tilde{\boldsymbol{x}}) = 0\}$. From Eqs. (84), (97) and (98), the nondimensional transport velocity $\tilde{\boldsymbol{v}}_{\boldsymbol{\tau}}(\tilde{\boldsymbol{x}}, \tilde{q})$ may be deduced as

$$\tilde{\boldsymbol{v}}_{\boldsymbol{\tau}}(\tilde{\boldsymbol{x}}, \tilde{q}) = \begin{bmatrix} -\dfrac{1}{a(\tilde{q})}\left(\tilde{a} + \tilde{x}\dfrac{\partial a(\tilde{q})}{\partial\tilde{q}}\right) & -\dfrac{\tilde{y}}{b(\tilde{q})}\dfrac{\partial b(\tilde{q})}{\partial\tilde{q}} \end{bmatrix}^{\mathrm{T}}. \tag{100}$$

It is worth observing that exactly the same diffeomorphism as in Eq. (97) may be used when considering the SDEC model proposed in [72, 74], provided that the *shape number* parameter ψ remains constant.

Finally, departing from the knowledge of the transformed state $\tilde{\boldsymbol{u}}_{\boldsymbol{\tau}}(\tilde{\boldsymbol{x}}, \tilde{q})$, the equilibrium relationships in Eq. (9) also yield[10]

$$\boldsymbol{F}_{\boldsymbol{\tau}}(q) = \iint_{\mathscr{C}(q)} \boldsymbol{p}_{\boldsymbol{\tau}}(\boldsymbol{x}, q)\,\mathrm{d}\boldsymbol{x} \equiv \iint_{\tilde{\mathscr{C}}} \tilde{\boldsymbol{p}}_{\boldsymbol{\tau}}(\tilde{\boldsymbol{x}}, \tilde{q})\big|\det\mathbf{J}_{\boldsymbol{\Xi}_{\tilde{x}}}(\tilde{\boldsymbol{x}}, \tilde{q})\big|\,\mathrm{d}\tilde{\boldsymbol{x}}$$
$$\triangleq \iint_{\tilde{\mathscr{C}}} \boldsymbol{p}_{\boldsymbol{\tau}}(\boldsymbol{x}, q)\bigg|_{(\boldsymbol{x}, q) = \boldsymbol{\Xi}(\tilde{\boldsymbol{x}}, \tilde{q})} \big|\det\mathbf{J}_{\boldsymbol{\Xi}_{\tilde{x}}}(\tilde{\boldsymbol{x}}, \tilde{q})\big|\,\mathrm{d}\tilde{\boldsymbol{x}}, \tag{101a}$$

$$M_z(q) = \iint_{\mathscr{C}(q)} x p_y(\boldsymbol{x}, q) - y p_x(\boldsymbol{x}, q)\,\mathrm{d}\boldsymbol{x}$$
$$\equiv \iint_{\tilde{\mathscr{C}}} \big(\Xi_{\tilde{x}}(\tilde{\boldsymbol{x}}, \tilde{q})\tilde{p}_y(\tilde{\boldsymbol{x}}, \tilde{q}) - \Xi_{\tilde{y}}(\tilde{\boldsymbol{x}}, \tilde{q})\tilde{p}_x(\tilde{\boldsymbol{x}}, \tilde{q})\big)\big|\det\mathbf{J}_{\boldsymbol{\Xi}_{\tilde{x}}}(\tilde{\boldsymbol{x}}, \tilde{q})\big|\,\mathrm{d}\tilde{\boldsymbol{x}} \tag{101b}$$
$$\triangleq \iint_{\tilde{\mathscr{C}}} \big(x p_y(\boldsymbol{x}, q) - y p_x(\boldsymbol{x}, q)\big)\bigg|_{(\boldsymbol{x}, q) = \boldsymbol{\Xi}(\tilde{\boldsymbol{x}}, \tilde{q})} \big|\det\mathbf{J}_{\boldsymbol{\Xi}_{\tilde{x}}}(\tilde{\boldsymbol{x}}, \tilde{q})\big|\,\mathrm{d}\boldsymbol{x},$$

where $\mathbf{J}_{\boldsymbol{\Xi}_{\tilde{x}}}(\tilde{\boldsymbol{x}}, \tilde{q})$ denotes the Jacobian matrix of the transformation $\boldsymbol{\Xi} : (\boldsymbol{x}, q) = \boldsymbol{\Xi}(\tilde{\boldsymbol{x}}, \tilde{q})$ with respect to the space coordinates. The formulae in Eq. (101) may be conveniently used to evaluate the transient forces and moment without inverting the mapping $\boldsymbol{\Phi} : (\tilde{\boldsymbol{x}}, \tilde{q}) = \boldsymbol{\Phi}(\boldsymbol{x}, q)$.

B   Derivation of the slip functions

Starting from simplified theory detailed in Sect. 4, the slip functions appearing in Eqs. (53) may be derived by differentiating the tangential forces and moment in Eqs. (9) with respect to time:

$$\dot{\boldsymbol{F}}_{\boldsymbol{\tau}}(t) = \iint_{\mathscr{C}} \frac{\partial\boldsymbol{p}_{\boldsymbol{\tau}}(\boldsymbol{x}, t)}{\partial t}\,\mathrm{d}\boldsymbol{x} = \mathbf{L}_{\boldsymbol{\tau}}^{-1} \iint_{\mathscr{C}} \frac{\partial\boldsymbol{u}_{\boldsymbol{\tau}}(\boldsymbol{x}, t)}{\partial t}\,\mathrm{d}\boldsymbol{x}, \tag{102a}$$

---

[10]It is worth mentioning that, since the solution lies in the space $L^\infty(\tilde{\mathscr{C}} \times (0, \tilde{Q}))$, the integrals defined in Eqs. (101) are actually finite concerning every domain of finite measure.

$$\dot{M}_z(t) = \iint_{\mathscr{C}} x \, \frac{\partial p_y(\boldsymbol{x}, t)}{\partial t} - y \, \frac{\partial p_x(\boldsymbol{x}, t)}{\partial t} \, \mathrm{d}\boldsymbol{x} = \iint_{\mathscr{C}} \frac{x}{L_y} \, \frac{\partial u_y(\boldsymbol{x}, t)}{\partial t} - \frac{y}{L_x} \, \frac{\partial u_x(\boldsymbol{x}, t)}{\partial t} \, \mathrm{d}\boldsymbol{x}. \tag{102b}$$

Assuming no-slip conditions ($\boldsymbol{s}(\boldsymbol{x}, t) = \boldsymbol{0}$), neglecting the partial derivative with respect to the longitudinal coordinate in Eq. (21) and substituting into (102) yields

$$\dot{\boldsymbol{F}}_{\boldsymbol{\tau}}(t) \approx -V(t)\mathbf{L}_{\boldsymbol{\tau}}^{-1} \iint_{\mathscr{C}} \left(\boldsymbol{\xi}(t) + \phi(t) \begin{bmatrix} -y \\ x \end{bmatrix} \right) \mathrm{d}\boldsymbol{x} = -V(t) \begin{bmatrix} A_{\mathscr{C}}\mathbf{L}_{\boldsymbol{\tau}}^{-1} & \mathbf{L}_{\boldsymbol{\tau}}^{-1}\tilde{\mathbf{I}}\boldsymbol{S}_{\mathscr{C}} \end{bmatrix} \begin{bmatrix} \boldsymbol{\xi}(t) \\ \phi(t) \end{bmatrix}, \tag{103a}$$

$$\dot{M}_z(t) \approx -V(t) \iint_{\mathscr{C}} \left[\frac{x}{L_y}\big(\xi_y(t) + \phi(t)x\big) - \frac{y}{L_x}\big(\xi_x(t) - \phi(t)y\big) \right] \mathrm{d}\boldsymbol{x} = \begin{bmatrix} \mathbf{I}_{\boldsymbol{\xi}} & I_\phi \end{bmatrix} \begin{bmatrix} \boldsymbol{\xi}(t) \\ \phi(t) \end{bmatrix}, \tag{103b}$$

where the following quantities have been defined:

$$A_{\mathscr{C}} \triangleq \iint_{\mathscr{C}} \mathrm{d}\boldsymbol{x}, \tag{104a}$$

$$\boldsymbol{S}_{\mathscr{C}} \triangleq \iint_{\mathscr{C}} \boldsymbol{x} \, \mathrm{d}\boldsymbol{x} \tag{104b}$$

$$\mathbf{I}_{\boldsymbol{\xi}} = \begin{bmatrix} I_{\xi_x} & I_{\xi_y} \end{bmatrix} \triangleq \begin{bmatrix} \iint_{\mathscr{C}} -\frac{y}{L_x} \, \mathrm{d}\boldsymbol{x} & \iint_{\mathscr{C}} \frac{x}{L_y} \, \mathrm{d}\boldsymbol{x} \end{bmatrix}, \tag{104c}$$

$$I_\phi \triangleq \iint_{\mathscr{C}} \frac{x^2}{L_y} + \frac{y^2}{L_x} \, \mathrm{d}\boldsymbol{x}, \tag{104d}$$

and the matrix $\tilde{\mathbf{I}}$ reads

$$\tilde{\mathbf{I}} \triangleq \begin{bmatrix} 0 & -1 \\ 1 & 0 \end{bmatrix}. \tag{105}$$

Equations (103) may be restated in matrix form as or

$$\begin{bmatrix} A_{\mathscr{C}}\mathbf{L}_{\boldsymbol{\tau}}^{-1} & \mathbf{L}_{\boldsymbol{\tau}}^{-1}\tilde{\mathbf{I}}\boldsymbol{S}_{\mathscr{C}} \\ \mathbf{I}_{\boldsymbol{\xi}} & I_\phi \end{bmatrix} \begin{bmatrix} \boldsymbol{\xi} \\ \phi \end{bmatrix} \approx -\frac{1}{V} \begin{bmatrix} \dot{\boldsymbol{F}}_{\boldsymbol{\tau}} \\ \dot{M}_z \end{bmatrix}. \tag{106}$$

Solving Eq. (106) for the creepages yields

$$\begin{bmatrix} \boldsymbol{\xi} \\ \phi \end{bmatrix} \approx \frac{1}{V} \begin{bmatrix} \check{\boldsymbol{\xi}}\big(\dot{\boldsymbol{F}}_{\boldsymbol{\tau}}, \dot{M}_z\big) \\ \check{\phi}\big(\dot{\boldsymbol{F}}_{\boldsymbol{\tau}}, \dot{M}_z\big) \end{bmatrix} \triangleq -\frac{1}{V} \begin{bmatrix} \mathbf{L}_{\boldsymbol{F}}' & \mathbf{L}_M' \\ \mathbf{L}_{\phi\boldsymbol{F}}' & L_{\phi M}' \end{bmatrix} \begin{bmatrix} \dot{\boldsymbol{F}}_{\boldsymbol{\tau}} \\ \dot{M}_z \end{bmatrix}, \tag{107}$$

where the matrix of generalised flexibilities is defined as

$$\begin{bmatrix} \mathbf{L}_{\boldsymbol{F}}' & \mathbf{L}_M' \\ \mathbf{L}_{\phi\boldsymbol{F}}' & L_{\phi M}' \end{bmatrix} \triangleq \begin{bmatrix} A_{\mathscr{C}}\mathbf{L}_{\boldsymbol{\tau}}^{-1} & \mathbf{L}_{\boldsymbol{\tau}}^{-1}\tilde{\mathbf{I}}\boldsymbol{S}_{\mathscr{C}} \\ \mathbf{I}_{\boldsymbol{\xi}} & I_\phi \end{bmatrix}^{-1}. \tag{108}$$

At low speed, the slip functions may be thus sought as follows:

$$\begin{bmatrix} \check{\boldsymbol{\xi}}\big(\dot{\boldsymbol{F}}_{\boldsymbol{\tau}}, \dot{M}_z\big) \\ \check{\phi}\big(\dot{\boldsymbol{F}}_{\boldsymbol{\tau}}, \dot{M}_z\big) \end{bmatrix} = - \begin{bmatrix} \mathbf{L}_{\boldsymbol{F}}' & \mathbf{L}_M' \\ \mathbf{L}_{\phi\boldsymbol{F}}' & L_{\phi M}' \end{bmatrix} \begin{bmatrix} \dot{\boldsymbol{F}}_{\boldsymbol{\tau}} \\ \dot{M}_z \end{bmatrix}, \tag{109}$$

where the matrix on the right-hand side is nonsingular, and $\mathbf{L}_{\boldsymbol{F}}'$, $\mathbf{L}_M'$, $\mathbf{L}_{\phi\boldsymbol{F}}'$ and $L_{\phi M}'$ represent generalised flexibilities. The system described by Eq. (109) is linear, and, as already anticipated, obviously admits a unique equilibrium in the origin [71], that is $[\check{\boldsymbol{\xi}}^{\mathrm{T}}(\boldsymbol{0}, 0) \; \check{\phi}(\boldsymbol{0}, 0)]^{\mathrm{T}} = [\boldsymbol{0}^{\mathrm{T}} \; 0]^{\mathrm{T}}$.

Furthermore, when the spin creepage ϕ and the spin moment M_z are neglected, Eq. (109) reduces to a relationship between the translational slip functions and the tangential forces in the form

$$\check{\boldsymbol{\xi}}\big(\dot{\boldsymbol{F}}_{\boldsymbol{\tau}}\big) = -\mathbf{L}_{\boldsymbol{F}}'\dot{\boldsymbol{F}}_{\boldsymbol{\tau}} = -\frac{1}{A_{\mathscr{C}}}\mathbf{L}_{\boldsymbol{\tau}}\dot{\boldsymbol{F}}_{\boldsymbol{\tau}}. \tag{110}$$

Clearly, since $\mathbf{L}_{\boldsymbol{\tau}}$ is diagonal and positive definite, $\mathbf{L}_{\boldsymbol{F}}'$ is also diagonal and positive definite.

It should be noticed that, in addition to disregarding the space derivative, another approximation has been introduced in the derivation of the slip functions: the integration over $\mathscr{C}$ has been performed assuming no-slip conditions. There is an obvious advantage in doing so, since this allows neglecting nonlinear effects arising at very low speed, which in turn implies that the slipping functions are also linear. This is a nice property of the system derived according to Eq. (109), which, as already mentioned, ensures the existence of a unique dynamical equilibrium in the origin [70, 71]. The assumption of no-slip conditions in the derivation of the slip function also regulates the rate of convergence towards the steady-state values of the tangential forces and spin moment, and may be adjusted *a posteriori* without affecting the properties of the model (as briefly mentioned in Sect. 7).